Journal of Quantitative Spectroscopy & Radiative Transfer 149 (2014) 318–333

Contents lists available at ScienceDirect

Journal of Quantitative Spectroscopy & Radiative Transfer

journal homepage: www.elsevier.com/locate/jqsrt

High resolution FTIR study of the $\nu_7+\nu_{10}-\nu_{10}$ and $\nu_{10}+\nu_{12}-\nu_{10}$ "hot" bands of C_2H_4

O.N. Ulenikov [a,*], O.V. Gromova [a], E.S. Bekhtereva [a], G.A. Onopenko [b], Yu.S. Aslapovskaya [a], K.-H. Gericke [c], S. Bauerecker [c], V.-M. Horneman [d]

[a] Institute of Physics and Technology, National Research Tomsk Polytechnic University, Tomsk 634050, Russia
[b] Department of Applied Mathematics, Tomsk State University of Architecture and Building, Tomsk 634003, Russia
[c] Institut für Physikalische und Theoretische Chemie, Technische Universität Braunschweig, D-38106 Braunschweig, Germany
[d] Department of Physics, Geology and Chemistry, P.O. Box 3000, FIN-90014 University of Oulu, Finland

ARTICLE INFO

Article history:
Received 16 June 2014
Received in revised form
20 August 2014
Accepted 21 August 2014
Available online 30 August 2014

Keywords:
Ethylene
High-resolution spectra
Spectroscopic parameters

ABSTRACT

Two weak "hot" absorption bands, $\nu_7+\nu_{10}-\nu_{10}$ and $\nu_{10}+\nu_{12}-\nu_{10}$, of ethylene, C_2H_4, were analyzed for the first time with high resolution using the Fourier transform interferometer Bruker IFS-120 HR. As the result of analysis we assigned about 930 and 370 transitions (404 and 185 upper state ro-vibrational energy values) with $J^{max.}=27$, $K_a^{max.}=14$ and $J^{max.}=20$, $K_a^{max.}=9$ for the bands $\nu_7+\nu_{10}-\nu_{10}$ and $\nu_{10}+\nu_{12}-\nu_{10}$, respectively. Strong local resonance interactions of the vibrational state ($\nu_{10}=\nu_{12}=1$) with the five other states, and of the state ($\nu_7=\nu_{10}=1$) with the seven other states were taken into account, and a set of 77 varied parameters, which reproduce the initial experimental data with the *rms* deviation of 6.1×10^{-4} cm^{-1} which is close to experimental uncertainties, was obtained.

1. Introduction

Ethylene is a naturally occurring compound in ambient air that affects atmospheric chemistry and the global climate. Ethylene acts as a hormone in plants and its role in plant biochemistry, physiology, mammal's metabolism, and ecology is the subject of extensive research. Due to its high reactivity towards hydroxyl (OH) radicals, ethylene plays a significant role in tropospheric chemistry [1] and ozone generation. This contribution to atmospheric chemistry makes ethylene a climate-relevant trace gas and its air concentration, sources and sinks are of interest to atmospheric science. Ethylene is one of the most relevant objects of study in astrophysics (see, *e.g.*, [2,3] and has been detected as a trace component of the atmospheres of the outer planets Jupiter, Saturn, Neptune [4–7], and the satellite Titan [8–13]. Ethylene has also been observed in circumstellar clouds IRC+10216 [2] and IRL618 [3]. Furthermore, ethylene is important as a prototype example in the development of our understanding of relating spectra, dynamics, and potential hypersurfaces of many organic molecules. Therefore, for many years, the ethylene molecule has been a subject of both extensive experimental (see, *e.g.* reviews in Refs. [14,15]), and theoretical (see, *e.g.*, Refs. [16,17] and references cited therein) studies.

Because of the D_{2h} symmetry of ethylene, three values $k_{z\alpha}$ ($\alpha=x,y$ or z)[1] are transformed in accordance with the

[1] It is known that the intensity of a line in the absence of an external field is proportional to $|\langle\alpha|P_z|\beta\rangle|$, where $\langle\alpha|$ and $|\beta\rangle$ represent the initial and final states of the molecule, respectively, and P_z is the component of the dipole moment along a spaced fixed axis Z. In this case, the P_z component is connected with the components μ_α, ($\alpha=x,y,z$) of the dipole moment along the molecular fixed axes by the following relation:

$$P_z=\sum_\alpha k_{z\alpha}\mu_\alpha.$$

* Corresponding author.
E-mail address: Ulenikov@mail.ru (O.N. Ulenikov).

http://dx.doi.org/10.1016/j.jqsrt.2014.08.013
0022-4073/

irreducible representations B_{2g}, B_{1g}, and B_{3g}, respectively, Ref. [18]. It means "cold" transitions (transitions from the ground vibrational state) are allowed in absorption only to the upper vibrational states of the symmetry B_{1u} (c-type transitions), B_{2u} (b-type transitions), and B_{3u} (a-type transitions). At the same time, belonging to the D_{2h} symmetry group, the C_2H_4 molecule possesses twelve vibrational modes and its vibrational states can be of eight different symmetries, A_g, A_u, $B_{\lambda g}$, and $B_{\lambda u}$ ($\lambda = 1, 2, 3$). This means that from eight possible on symmetry types of vibrational bands, only three ones can be realized for the mostly accurate and informative "cold" absorption bands. Moreover, knowledge of rotational structures of other types of excited vibrational states (in particular, vibrational states of *g*-type symmetries: A_g, B_{1g}, B_{2g}, and B_{3g}) is very important for applications in different problems of physics and physical chemistry. The only way for extraction of information about *g*-type excited vibrational states of C_2H_4 from absorption spectra is the study of "hot" transitions (of course, the *g*-type upper states can be studied also by the Raman spectroscopy, see, *e.g.*, Refs. [19–21]).

"Hot" bands of C_2H_4 have been analyzed in the spectroscopic literature several times. In Ref. [22] spectroscopic information about the "hot" band $\nu_7 - \nu_8$ was summarized, and parameters of the $(\nu_8 = 1, B_{2g})$ band were obtained. A double resonance technique was used in Ref. [23] for the study of "hot" bands $\nu_9 + \nu_{10} - \nu_{10}$ and $\nu_7 + \nu_9 - \nu_7$. The "hot" bands $\nu_7 + \nu_9 - \nu_7$, $\nu_{10} + \nu_{11} - \nu_{10}$ and $\nu_7 + \nu_{11} - \nu_7$ were considered also in Ref. [24]. In the present study we analyze the rotational structure of the lowest "hot" bands of C_2H_4 which are caused by transitions from the vibrational state $(\nu_{10} = 1, B_{2u})$ to the set of corresponding lowest on energy vibrational state $(\nu_7 = \nu_{10} = 1, B_{3g})$, $(\nu_{10} = \nu_{12} = 1, B_{1g})$, and $(\nu_{10} = 2, A_g)$. The rotational structure of the $(\nu_{10} = 2, A_g)$ vibrational state was analyzed earlier a few times in Raman spectroscopy, Refs. [19–21]. On that reason we focus our attention to the couple of states $(\nu_7 = \nu_{10} = 1, B_{3g})$ and $(\nu_{10} = \nu_{12} = 1, B_{1g})$ which means the absorption bands $\nu_7 + \nu_{10} - \nu_{10}$ and $\nu_{10} + \nu_{12} - \nu_{10}$. These "hot" bands (and corresponding upper vibrational states $(\nu_7 = \nu_{10} = 1, B_{3g})$ and $(\nu_{10} = \nu_{12} = 1, B_{1g})$) are analyzed in the present study for the first time. The experimental details of our study are discussed in Section 2. In Section 3 we briefly discuss the theoretical background of further fitting the obtained data. Description of the recorded spectrum, assignments of transitions, and determination of upper ro-vibrational energies are presented in Section 4. The final Section 5 presents the results of theoretical analysis of the obtained upper ro-vibrational energies and determination of spectroscopic parameters of the model.

2. Experimental details

The experimental spectra in the region of 800–1130 cm^{-1} and 1360–1540 cm^{-1} were recorded with Bruker IFS-120HR Fourier transform interferometer in the Infrared Laboratories of University of Oulu and of Technische Universität Braunschweig, respectively. A globar source, KBr beamsplitter and a mercury-cadmium-telluride semiconductor detector were used at both places. The C_2H_4 sample, made by Linde AG, with a purity of 99.99%, was studied by an absorption spectroscopic method in multipath White cells in Oulu, Ref. [25], and Braunschweig, Ref. [26].

For the 800–1130 cm^{-1} region two spectra have been recorded at room temperature: one with 0.1 Pa, 48 m absorption path length, 1636 scans over 80.8 h (Oulu, shown in Fig. 1) and the other with 50 Pa, 8 m absorption path length, 500 scans over 25 h (Braunschweig). For the 1360–1540 cm^{-1} region three spectra have been recorded:

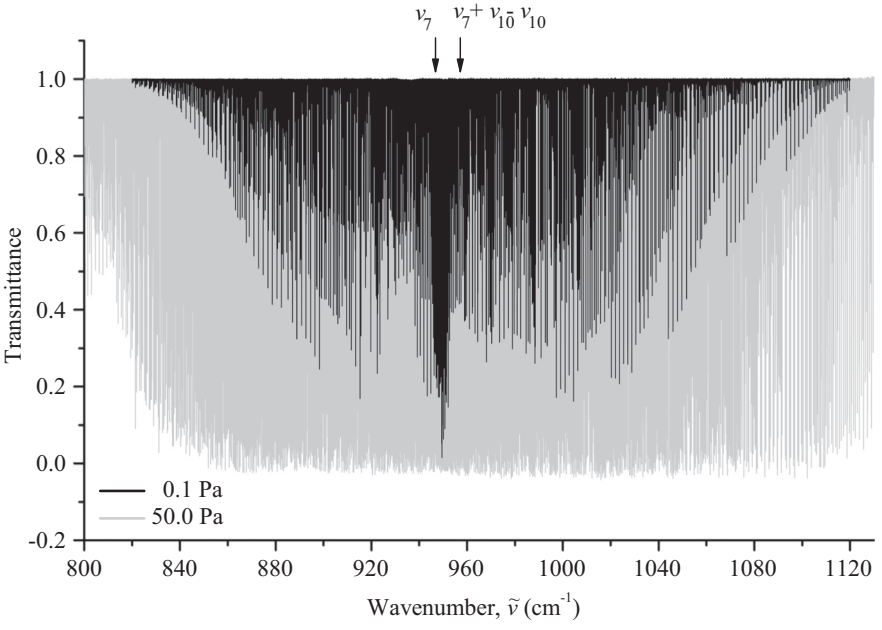

Fig. 1. Survey spectrum of C_2H_4 in the region of the $\nu_7 + \nu_{10} - \nu_{10}$ "hot" band. Experimental conditions: sample pressure is 0.1 Pa, absorption path length is 48 m; room temperature; number of scans is 1636 for the "grey" spectrum; sample pressure is 50 Pa, absorption path length is 8 m, temperature is 298 K, number of scans is 500 for the "black" spectrum.

one at room temperature, 13 Pa, 48 m absorption path length, 1794 scans over 63.3 h (Oulu, shown in Fig. 2) and the two other spectra at 298 K and 350 K, 50 Pa and 200 Pa, 570 (28 h) and 500 scans (25 h), and 8 m optical path length each (Braunschweig). The Oulu spectra were calibrated with peaks of the CO_2 ν_2 band ($\nu_0 =$ 667.3799154(13) cm^{-1}), Ref. [27]. The peak positions were calculated with the optimized center of gravity method discussed in Ref. [28]. The Braunschweig spectra were calibrated with N_2O lines of the 1130–1330 cm^{-1} and 1330–1346 cm^{-1} band regions. The peak positions were also calculated with the optimized center of gravity method discussed in Ref. [29].

The final spectral resolution was mainly limited by Doppler broadening and resulted in 0.003 cm^{-1} for the ν_7 region around 950 cm^{-1} and 0.004 cm^{-1} for the ν_{12} region around 1440 cm^{-1}. An instrumental resolution of 0.0025 cm^{-1} (Braunschweig) and 0.0020 cm^{-1} (Oulu) was used for these regions. The wavenumber accuracy of non-blended, unsaturated and not too weak lines can be estimated to be better than 10^{-4} cm^{-1} in both the regions.

3. Hamiltonian model

The C_2H_4 molecule is an asymmetric top with the value of the asymmetry parameter $\kappa = (2B-A-C)/(A-C) \approx -0.915$ and with the symmetry isomorphic to the D_{2h} point symmetry group (see Fig. 3). As a consequence, twelve vibrational modes of C_2H_4 possess the symmetries which are shown in the column 11 of Table 1. Also, in accordance with the symmetry of the molecule, three $k_{z\alpha}$ values, k_{zx}, k_{zy}, and k_{zz}, are transformed in accordance with the irreducible representations, B_{2g}, B_{1g}, and B_{3g}, respectively. It means, only transitions between the vibrational states $|v\Gamma\rangle$ and $|\tilde{v}\tilde{\Gamma}\rangle$, for which

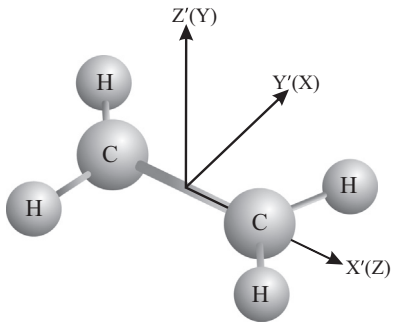

Fig. 3. Axes definitions used in the present work for the ethylene, C_2H_4, molecule. The primed symbols refer to the axis definitions for the D_{2h} symmetry group used in the classification of the vibrational modes. The unprimed symbols refer to the Cartesian axis definitions of the I^r representation of Watson's *A*-reduced effective Hamiltonian.

Table 1
Symmetry types and characters of irreducible representations of the D_{2h} group.

Repr. 1	*E* 2	$\sigma_{x'y'}$ 3	$\sigma_{x'z'}$ 4	$\sigma_{y'z'}$ 5	*i* 6	$C_2(z')$ 7	$C_2(y')$ 8	$C_2(x')$ 9	Rot. 10	Vibr. 11
A_g	1	1	1	1	1	1	1	1		q_1, q_2, q_3
A_u	1	−1	−1	−1	−1	1	1	1		q_4
B_{1g}	1	1	−1	−1	1	1	−1	−1	J_y, k_{zy}	q_5, q_6
B_{1u}	1	−1	1	1	−1	1	−1	−1		q_7
B_{2g}	1	−1	1	−1	1	−1	1	−1	J_x, k_{zx}	q_8
B_{2u}	1	1	−1	1	−1	−1	1	−1		q_9, q_{10}
B_{3g}	1	−1	−1	1	1	−1	−1	1	J_z, k_{zz}	
B_{3u}	1	1	1	−1	−1	−1	−1	1		q_{11}, q_{12}

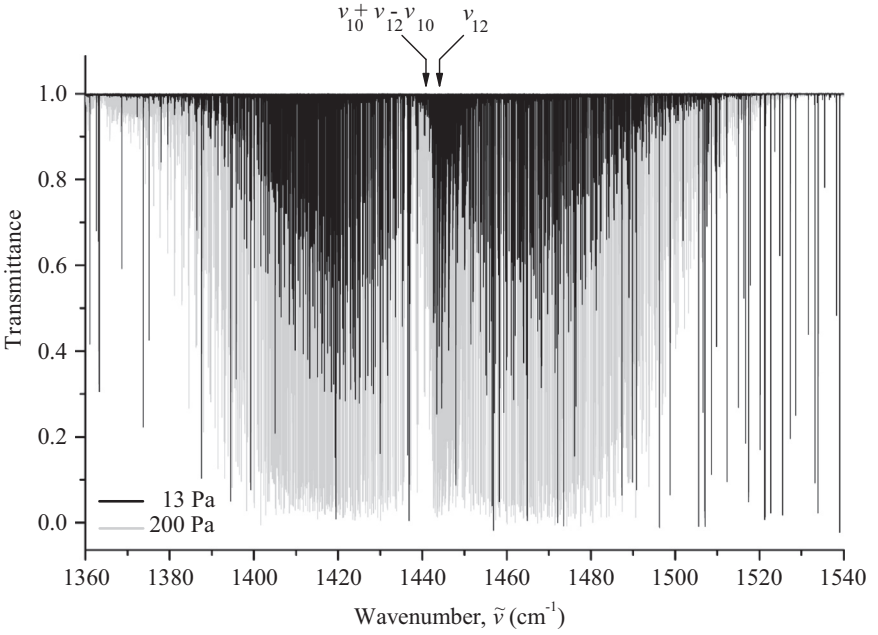

Fig. 2. Survey spectrum of C_2H_4 in the region of the of the $\nu_{10}+\nu_{12}-\nu_{10}$ "hot" band. Experimental conditions: sample pressure is 13 Pa, absorption path length is 48 m; room temperature; number of scans is 1794 for the "grey" spectrum; sample pressure is 200 Pa, absorption path length is 8 m, temperature is 350 K, number of scans is 500 for the "black" spectrum.

the relation

$$\Gamma \otimes \tilde{\Gamma} = A_u \otimes \gamma^{\alpha} \quad (1)$$

is fulfilled, are possible (here Γ and $\tilde{\Gamma}$ are the symmetries of the wave functions $|v\Gamma\rangle$ and $|\tilde{v}\tilde{\Gamma}\rangle$, respectively; γ^{α} is a symmetry of $k_{z\alpha}$; the $\otimes$ denotes a tensorial product). For the "cold" bands it means that transitions are allowed from the ground vibrational state (A_g symmetry) to the upper vibrational states of the symmetry B_{1u} (c-type transitions), B_{2u} (b-type transitions), and B_{3u} (a-type transitions). Because the lowest vibrational state of the u-type symmetry is $(v_{10}=1, A_u)$, one can expect at the same time in accordance with Eq. (1), that the lowest "hot" bands which can appear in absorbance are the bands $\nu_7+\nu_{10}-\nu_{10}$ ($B_{1u}-$ type), $\nu_{10}+\nu_{12}-\nu_{10}$ ($B_{3u}-$ type), and $2\nu_{10}-\nu_{10}$ ($B_{2u}-$ type). Corresponding upper vibrational states are $(v_7=v_{10}=1, B_{3g})$, $(v_{10}=v_{12}=1, B_{1g})$, and $(v_{10}=2, A_g)$. As follows from Ref. [17], the states $(v_7=v_{10}=1, B_{3g})$ and $(v_{10}=v_{12}=1, B_{1g})$ which are considered in the present study may strongly interact with a whole set of doubly excited vibrational states: $(v_{10}=2, A_g)$, $(v_4=2, A_g)$, $(v_7=2, A_g)$, $(v_{12}=2, A_g)$, $(v_4=v_7=1, B_{1g})$, $(v_4=v_{10}=1, B_{2g})$, $(v_4=v_{12}=1, B_{3g})$, $(v_7=v_{12}=1, B_{2g})$. Moreover, two additional states, $(v_3=v_8=1, B_{2g})$ and $(v_8=2, A_g)$, which are located very close to the states $(v_{10}=v_{12}=1, B_{1g})$ and $(v_4=v_{10}=1, B_{2g})$, respectively, and can influence rotational structures of the states $(v_7=v_{10}=1, B_{3g})$ and $(v_{10}=v_{12}=1, B_{1g})$, were taken into account in our analysis:

(a) the state $(v_{10}=v_{12}=1, B_{1g})$ interacts with the state $(v_3=v_8=1, B_{2g})$ through strong interaction between $(v_3=v_8=1, B_{2g})$ and $(v_7=v_{12}=1, B_{2g})$ (difference between unperturbed vibrational energies, $\Delta E = E_{(v_3=v_8=1, B_{2g})} - E_{(v_{10}=v_{12}=1, B_{1g})}$, is less then 10 cm^{-1}), and

(b) the state $(v_4=v_{10}=1, B_{2g})$ strongly interacts with the state $(v_8=2, A_g)$ (difference between unperturbed vibrational energies, $\Delta E = E_{(v_8=2, A_g)} - E_{(v_4=v_{10}=1, B_{2g})}$, is about 15 cm^{-1}).

At the same time, taking into account that the vibrational state $(v_{10}=v_{12}=1, B_{1g})$ is located far enough from the states $(v_{10}=2, A_g)$, $(v_4=v_{10}=1, B_{2g})$, and $(v_7=v_{10}=1, B_{3g})$ and to make analysis not too complicate, we did not consider interactions between the state $(v_{10}=v_{12}=1, B_{1g})$, on the one hand, and the states $(v_{10}=2, A_g)$, $(v_4=v_{10}=1, B_{2g})$, and $(v_7=v_{10}=1, B_{3g})$, on the other hand.

As is seen from the above discussion, we consider here only the vibrational states of the g-type symmetry, A_g, B_{1g}, B_{2g}, and B_{3g}. This follows from the fact (see column 10 of Table 1) that any of three rotational operators $J_{\alpha}(\alpha=x,y,z)$ is transformed in accordance with the g-type irreducible representation of the D_{2h} group. As a consequence, only vibrational states of g-type, or only vibrational states of u-type can interact with each other. Following the above said, we used in our present study the Hamiltonian model of asymmetric top molecule in its mostly general form (for more details see, *e.g.*, Refs. [30–36]),

$$H^{vib.-rot.} = \sum_{v,\tilde{v}} |v\rangle\langle\tilde{v}| H^{v\tilde{v}}, \quad (2)$$

where the summation is taken from 1 to 12 for both v and $\tilde{v}$, which represent the ten vibrational states mentioned above:

A_g-symmetry: $|1\rangle=(v_{10}=2)$, $|2\rangle=(v_8=2)$, $|3\rangle=(v_7=2)$, $|4\rangle=(v_4=2)$, $|5\rangle=(v_{12}=2)$
B_{2g}-symmetry: $|6\rangle=(v_4=v_{10}=1)$, $|7\rangle=(v_3=v_8=1)$, $|8\rangle=(v_7=v_{12}=1)$
B_{3g}-symmetry: $|9\rangle=(v_7=v_{10}=1)$, $|10\rangle=(v_4=v_{12}=1)$
B_{1g}-symmetry: $|11\rangle=(v_4=v_7=1)$, $|12\rangle=(v_{10}=v_{12}=1)$.

Any of the diagonal blocks H^{vv}, Eq. (2), describes unperturbed rotational structure of the vibrational state $|v\rangle$ and has a form of reduced effective Hamiltonian in the A-reduction and I^r representation (see, *e.g.*, Refs. [37,38]):

$$\begin{aligned} H_{vv} = {} & E^v + \left[A^v - \frac{1}{2}(B^v + C^v)\right] J_z^2 + \frac{1}{2}(B^v + C^v) J^2 + \frac{1}{2}(B^v - C^v) J_{xy}^2 \\ & - \Delta_K^v J_z^4 - \Delta_{JK}^v J_z^2 J^2 - \Delta_J^v J^4 - \delta_K^v \left[J_z^2, J_{xy}^2\right]_+ - 2\delta_J^v J^2 J_{xy}^2 \\ & + H_K^v J_z^6 + H_{KJ}^v J_z^4 J^2 + H_{JK}^v J_z^2 J^4 + H_J^v J^6 + \left[J_{xy}^2, h_K^v J_z^4 \right. \\ & \left. + h_{JK}^v J^2 J_z^2 + h_J^v J^4\right]_+ + L_K^v J_z^8 + L_{KKJ}^v J_z^6 J^2 + L_{JK}^v J_z^4 J^4 \\ & + L_{KJJ}^v J_z^2 J^6 + L_J^v J^8 + \left[J_{xy}^2, l_K^v J_z^6 + l_{KJ}^v J^2 J_z^4 + l_{JK}^v J^4 J_z^2 + l_J^v J^6\right]_+ + \cdots, \end{aligned} \quad (3)$$

where $J_{xy}^2 = J_x^2 - J_y^2$; $[\cdots,\cdots]_+$ denotes anticommutator; A^v, B^v, and C^v are the effective rotational constants connected with the vibrational states (v), and the other parameters are the different order centrifugal distortion coefficients. Nondiagonal blocks $H^{v\tilde{v}}$ $(v \neq \tilde{v})$ describe four different kinds of resonance interactions between vibrational states of g-type symmetries. In this case, the operators $H^{v\tilde{v}}$ which connect the vibrational states $|v\Gamma_g\rangle$ and $|\tilde{v}\Gamma_g\rangle$ of the same symmetry Γ_g are the operators of the Fermi-type and they have a form:

$$\begin{aligned} H_{v\tilde{v}} = {} & {}^{v\tilde{v}}F_0 + {}^{v\tilde{v}}F_K J_z^2 + {}^{v\tilde{v}}F_J J^2 + {}^{v\tilde{v}}F_{KK} J_z^4 + {}^{v\tilde{v}}F_{KJ} J_z^2 J^2 + {}^{v\tilde{v}}F_{JJ} J^4 + \ldots \\ & + {}^{v\tilde{v}}F_{xy}\left(J_x^2 - J_y^2\right) + {}^{v\tilde{v}}F_{Kxy}\left[J_z^2, \left(J_x^2 - J_y^2\right)\right]_+ \\ & + {}^{v\tilde{v}}F_{Jxy} J^2 \left(J_x^2 - J_y^2\right) + \cdots \end{aligned} \quad (4)$$

The first parameter in Eq. (4), ${}^{v\tilde{v}}F_0$, is a pure vibrational interaction term; all the other parameters describe rotation–vibration part of Fermi-interaction.

A Coriolis-type interactions are presented in the Hamiltonian, Eq. (2), by the three different operators in which the main parts (proportional to iJ_x, iJ_y, and iJ_z) are transformed in accordance with the irreducible representations B_{2g}, B_{1g}, and B_{3g} of the D_{2h} group, respectively. In this case, if $(|v\Gamma_g\rangle \otimes |v\tilde{\Gamma}_g\rangle = B_{1g})$, then interaction operator can be written as

$$\begin{aligned} H_{v\tilde{v}} = {} & iJ_y H_{v\tilde{v}}^{(1)} + H_{v\tilde{v}}^{(1)} iJ_y + [J_x, J_z]_+ H_{v\tilde{v}}^{(2)} + H_{v\tilde{v}}^{(2)} [J_x, J_z]_+ \\ & + \left[iJ_y, \left(J_x^2 - J_y^2\right)\right]_+ H_{v\tilde{v}}^{(3)} + H_{v\tilde{v}}^{(3)} \left[iJ_y, \left(J_x^2 - J_y^2\right)\right]_+ + \cdots \end{aligned} \quad (5)$$

When $(|v\Gamma_g\rangle \otimes |v\tilde{\Gamma}_g\rangle = B_{2g})$, the corresponding Coriolis-interaction operator has the form

$$\begin{aligned} H_{v\tilde{v}} = {} & iJ_x H_{v\tilde{v}}^{(1)} + H_{v\tilde{v}}^{(1)} iJ_x + [J_y, J_z]_+ H_{v\tilde{v}}^{(2)} + H_{v\tilde{v}}^{(2)} [J_y, J_z]_+ \\ & + \left[iJ_x, \left(J_x^2 - J_y^2\right)\right]_+ H_{v\tilde{v}}^{(3)} + H_{v\tilde{v}}^{(3)} \left[iJ_x, \left(J_x^2 - J_y^2\right)\right]_+ + \cdots \end{aligned} \quad (6)$$

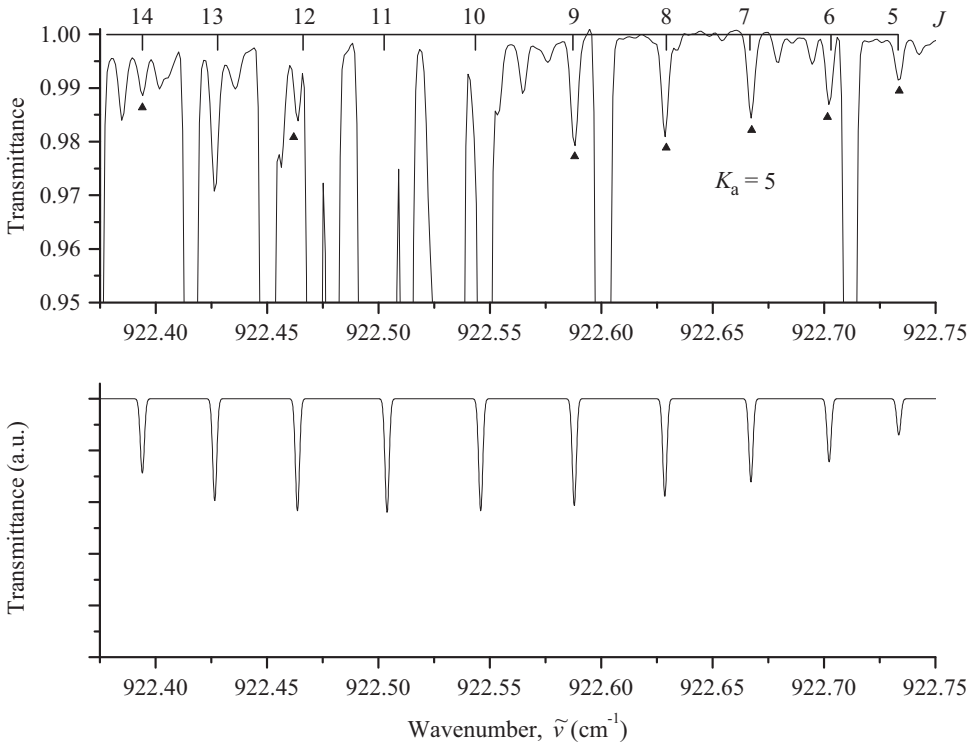

Fig. 4. A small part of the high resolution experimental spectrum of C_2H_4 (upper part of the figure) in the region of Q-branch of the $\nu_7+\nu_{10}-\nu_{10}$ band. Experimental conditions correspond to the "weak" spectrum: sample pressure, 0.1 Pa; absorption path length, 48 m; room temperature; 1636 scans. Transitions, $[J\ K_a=4K_c]\leftarrow[J'=J\ K'_a=5K'_c]$, assigned to the $\nu_7+\nu_{10}-\nu_{10}$ band are marked by the dark triangles. Unmarked lines belong to the strong ν_7 band. The bottom part presents the simulated spectrum of the $\nu_7+\nu_{10}-\nu_{10}$ band in the shown region.

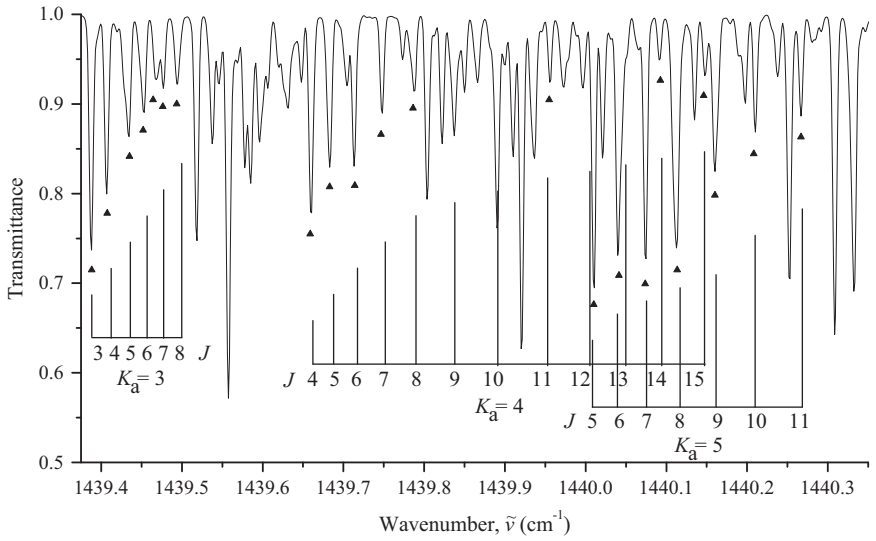

Fig. 5. A small part of the high resolution spectrum of the C_2H_4 molecule in the region of Q-branch of the $\nu_{10}+\nu_{12}-\nu_{10}$ band. Experimental conditions: sample pressure, 13 Pa; absorption path length, 48 m; room temperature; 1794 scans. Three sets of transitions, $[J\ K_aK_c]\leftarrow[J'=J\ K'_a=K_aK'_c]$, assigned to the $\nu_{10}+\nu_{12}-\nu_{10}$ band are marked by the dark triangles. Unmarked lines belong to the strong ν_{12} band.

In the third case, when $(|v\Gamma_g\rangle\otimes|v\tilde{\Gamma}_g\rangle=B_{3g}$, the Coriolis-interaction operator is

$$H_{v\tilde{v}}=iJ_zH^{(1)}_{v\tilde{v}}+[J_x,J_y]_+H^{(2)}_{v\tilde{v}}+H^{(2)}_{v\tilde{v}}[J_x,J_y]_+ + \left[iJ_z,\left(J_x^2-J_y^2\right)\right]_+H^{(3)}_{v\tilde{v}}+H^{(3)}_{v\tilde{v}}\left[iJ_z,\left(J_x^2-J_y^2\right)\right]_+ +\cdots \qquad (7)$$

The values $H^{(i)}_{v\tilde{v}}$ $(i=1,2,3)$ in Eqs. (6)–(8) are also operators, and they can be written in a general form as

$$H^{(i)}_{v\tilde{v}}=\frac{1}{2}{}^{v\tilde{v}}C^i+{}^{v\tilde{v}}C^i_KJ_z^2+\frac{1}{2}{}^{v\tilde{v}}C^i_JJ^2 +{}^{v\tilde{v}}C^i_{KK}J_z^4+{}^{v\tilde{v}}C^i_{KJ}J_z^2J^2+\frac{1}{2}{}^{v\tilde{v}}C^i_{JJ}J^4$$

Table 2
Statistical information for the $\nu_7+\nu_{10}-\nu_{10}$ and $\nu_{10}+\nu_{12}-\nu_{10}$ bands of the C_2H_4 molecule.

Band 1	Center/cm^{-1} 2	$J^{max.}$ 3	$K_a^{max.}$ 4	N_t[a] 5	N_l[b] 6	*rms* 7	m_1[c] 8	m_2[c] 9	m_3[c] 10
$\nu_7+\nu_{10}-\nu_{10}$	955.0821	27	14	929	404	5.4	68.1	17.8	14.1
$\nu_{10}+\nu_{12}-\nu_{10}$	1439.0381	20	9	376	185	7.9	53.0	25.9	21.1

[a] N_t is the numbers of transitions.
[b] N_l is the numbers of upper levels.
[c] Here $m_i = n_i/N \times 100\%$ ($i=1, 2, 3$); n_1, n_2, and n_3 are the numbers of levels (transitions) for which the differences $\delta = E^{exp.} - E^{calc.}$ ($\delta = \nu^{exp} - \nu^{calc}$) satisfy the conditions $\delta \le 3\times10^{-4}$ cm^{-1}, 3×10^{-4} cm$^{-1} < \delta \le 6\times10^{-4}$ cm^{-1}, and $\delta > 6\times10^{-4}$ cm^{-1}.

Table 3
Small part of the list of assigned transitions in the $\nu_7+\nu_{10}-\nu_{10}$ "hot" bands of C_2H_4.

Wavenumber (cm^{-1}) 1	J	K_a 2	K_c	J'	K'_a 3	K'_c	Transmit (%) 4	$\delta\times10^4$ (cm^{-1}) 5	Band 6	Spectrum 7
956.3723	10	1	10	10	0	10	95.5	0	$\nu_7+\nu_{10}-\nu_{10}$	I
956.5633	20	2	19	20	1	19	8.2	−9	$\nu_7+\nu_{10}-\nu_{10}$	II
956.6409	9	1	9	9	0	9	95.8	0	$\nu_7+\nu_{10}-\nu_{10}$	I
956.9129	19	2	18	19	1	18	14.7	−3	$\nu_7+\nu_{10}-\nu_{10}$	II
956.9478	8	1	8	8	0	8	96.1	−2	$\nu_7+\nu_{10}-\nu_{10}$	I
957.2825	7	1	7	7	0	7	96.8	−3	$\nu_7+\nu_{10}-\nu_{10}$	I
957.3396	18	2	17	18	1	17	4.2	0	$\nu_7+\nu_{10}-\nu_{10}$	II
957.6297	6	1	6	6	0	6	97.3	−5	$\nu_7+\nu_{10}-\nu_{10}$	I
957.8453	17	2	16	17	1	16	10.6	4	$\nu_7+\nu_{10}-\nu_{10}$	II
958.4261	16	2	15	16	1	15	3.0	5	$\nu_7+\nu_{10}-\nu_{10}$	II
959.0738	15	2	14	15	1	14	13.9	5	$\nu_7+\nu_{10}-\nu_{10}$	II
960.5139	13	2	12	13	1	12	9.3	−2	$\nu_7+\nu_{10}-\nu_{10}$	II
961.2727	12	2	11	12	1	11	3.2	4	$\nu_7+\nu_{10}-\nu_{10}$	II
962.0317	11	2	10	11	1	10	9.0	−1	$\nu_7+\nu_{10}-\nu_{10}$	II
962.7748	10	2	9	10	1	9	96.0	−2	$\nu_7+\nu_{10}-\nu_{10}$	I
963.5683	20	3	18	20	2	18	17.3	−2	$\nu_7+\nu_{10}-\nu_{10}$	II
964.1542	8	2	7	8	1	7	96.7	−1	$\nu_7+\nu_{10}-\nu_{10}$	I
964.7280	19	3	17	19	2	17	31.1	5	$\nu_7+\nu_{10}-\nu_{10}$	II
964.7675	7	2	6	7	1	6	98.6	2	$\nu_7+\nu_{10}-\nu_{10}$	I
964.8725	3	1	2	2	0	2	99.1	2	$\nu_7+\nu_{10}-\nu_{10}$	I
965.8944	18	3	16	18	2	16	10.6	−9	$\nu_7+\nu_{10}-\nu_{10}$	II
966.5340	3	2	2	3	1	2	99.3	−2	$\nu_7+\nu_{10}-\nu_{10}$	I
966.7829	2	2	1	2	1	1	99.1	−1	$\nu_7+\nu_{10}-\nu_{10}$	I
966.9707	4	1	3	3	0	3	99.0	1	$\nu_7+\nu_{10}-\nu_{10}$	I
967.0518	17	3	15	17	2	15	26.4	−1	$\nu_7+\nu_{10}-\nu_{10}$	II
968.1794	16	3	14	16	2	14	9.7	7	$\nu_7+\nu_{10}-\nu_{10}$	II
969.1557	5	1	4	4	0	4	98.7	−9	$\nu_7+\nu_{10}-\nu_{10}$	I
969.2583	15	3	13	15	2	13	7.9	0	$\nu_7+\nu_{10}-\nu_{10}$	II
970.2754	14	3	12	14	2	12	17.9	8	$\nu_7+\nu_{10}-\nu_{10}$	II
970.5658	2	2	0	1	1	0	98.9	−8	$\nu_7+\nu_{10}-\nu_{10}$	I
970.7197	2	2	1	1	1	1	98.5	−2	$\nu_7+\nu_{10}-\nu_{10}$	I
971.4429	6	1	5	5	0	5	98.9	−2	$\nu_7+\nu_{10}-\nu_{10}$	I
972.0625	12	3	10	12	2	10	25.1	7	$\nu_7+\nu_{10}-\nu_{10}$	II
972.2214	3	2	1	2	1	1	98.1	2	$\nu_7+\nu_{10}-\nu_{10}$	I
972.6723	3	2	2	2	1	2	99.3	−1	$\nu_7+\nu_{10}-\nu_{10}$	I
972.8097	11	3	9	11	2	9	15.6	4	$\nu_7+\nu_{10}-\nu_{10}$	II
973.4493	10	3	8	10	2	8	16.3	8	$\nu_7+\nu_{10}-\nu_{10}$	II
973.8165	4	2	2	3	1	2	85.0	−1	$\nu_7+\nu_{10}-\nu_{10}$	I
973.8438	7	1	6	6	0	6	98.8	−2	$\nu_7+\nu_{10}-\nu_{10}$	I
973.9772	9	3	7	9	2	7	22.7	6	$\nu_7+\nu_{10}-\nu_{10}$	II
974.3961	8	3	6	8	2	6	22.1	5	$\nu_7+\nu_{10}-\nu_{10}$	II
974.6980	4	2	3	3	1	3	98.2	−2	$\nu_7+\nu_{10}-\nu_{10}$	I
974.7135	7	3	5	7	2	5	27.3	2	$\nu_7+\nu_{10}-\nu_{10}$	II
974.9422	6	3	4	6	2	4	24.0	3	$\nu_7+\nu_{10}-\nu_{10}$	II
975.0976	5	3	3	5	2	3	99.2	2	$\nu_7+\nu_{10}-\nu_{10}$	I
975.1965	4	3	2	4	2	2	99.5	0	$\nu_7+\nu_{10}-\nu_{10}$	I

Table 4
Ro-vibrational term values for the ($v_7 = v_{10} = 1$) vibrational state of the C_2H_4 molecule (in cm^{-1})[a].

J	K_a 1	K_c	E 2	Δ 3	δ 4	J	K_a 1	K_c	E 2	Δ 3	δ 4	J	K_a 1	K_c	E 2	Δ 3	δ 4
0	0	0	1781.0089		10	7	1	6	1837.4653	2	−1	9	9	0	2181.7242	2	0
1	0	1	1782.8136	1	−1	7	2	6	1847.2672	2	0	10	0	10	1878.4426	1	0
1	1	0	1786.8288		−1	7	2	5	1847.7819	1	2	10	1	10	1879.7452	1	0
2	0	2	1786.4214		0	7	3	5	1867.1108	4	3	10	1	9	1887.7930	2	−5
2	1	1	1790.5892	1	−1	7	3	4	1867.1264	2	3	10	2	9	1895.7821	1	−1
2	2	1	1802.1899	1	−1	7	4	4	1894.6727	2	2	10	2	8	1897.6648	5	6
2	2	0	1802.1935		−7	7	4	3	1894.6727	2	1	10	3	8	1916.0150	3	5
3	0	3	1791.8224	2	−1	7	5	3	1930.1345	2	1	10	3	7	1916.1406	4	6
3	1	2	1796.2272	2	1	7	5	2	1930.1345	2	1	10	4	7	1943.5262	4	5
3	2	2	1807.6071	2	−1	7	7	1	2024.7492	3	2	10	5	6	1978.9339	3	0
3	2	1	1807.6282	2	1	7	7	0	2024.7492	3	2	10	5	5	1978.9339	3	1
3	3	1	1827.3185	3	−1	8	0	8	1845.1754	2	−4	10	6	5	2022.2426	2	−9
3	3	0	1827.3185	3	−2	8	1	8	1847.0969		−2	10	6	4	2022.2426	2	−9
4	0	4	1799.0039	3	−4	8	1	7	1852.4118	1	0	10	7	4	2073.4160	1	2
4	1	3	1803.7389	1	0	8	2	7	1861.6601	1	−1	10	7	3	2073.4160	1	2
4	2	3	1814.8268	2	0	8	2	6	1862.5030	2	3	10	8	3	2132.0528	3	−4
4	2	2	1814.8896	2	0	8	3	6	1881.5948	2	4	10	8	2	2132.0528	3	−4
4	3	2	1834.5488	3	1	8	3	5	1881.6291	3	5	10	9	2	2199.8598	2	−2
4	3	1	1834.5488	3	−3	8	4	5	1909.1414	3	4	10	9	1	2199.8598	2	−2
4	4	1	1862.1385	1	−1	8	4	4	1909.1417	3	4	10	10	1	2274.6392	7	2
4	4	0	1862.1385	1	−1	8	5	4	1944.5893	2	1	10	10	0	2274.6392	7	2
5	0	5	1807.9505	2	−2	8	5	3	1944.5893	2	1	11	0	11	1897.5626	1	0
5	1	4	1813.1206		3	8	6	3	1987.9348	2	−2	11	1	11	1898.6057	5	−3
5	2	4	1823.8458		−1	8	6	2	1987.9348	2	−2	11	1	10	1908.1975		−3
5	2	3	1823.9917	1	0	8	7	2	2039.1649	1	0	11	2	10	1915.4981	2	0
5	3	3	1843.5894	2	0	8	7	1	2039.1649	1	0	11	2	9	1918.1195	4	6
5	3	2	1843.5910	5	−5	8	8	1	2098.1194	2	2	11	3	9	1935.9518	4	4
5	4	2	1871.1731	2	1	8	8	0	2098.1194	2	2	11	3	8	1936.1699	4	9
5	4	1	1871.1731	2	1	9	0	9	1860.9760		−3	11	4	8	1963.4467	3	4
5	5	1	1906.6529	2	−2	9	1	9	1862.5736	2	−1	11	4	7	1963.4534	4	−18
5	5	0	1906.6529	2	−2	9	1	8	1869.1924	2	−2	11	5	7	1998.8269	2	−2
6	0	6	1818.6421	1	−1	9	2	8	1877.8339	1	0	11	5	6	1998.8269	2	0
6	1	6	1821.2512		−5	9	2	7	1879.1269	5	−1	11	6	6	2042.1115	2	−21
6	1	5	1824.3649	1	−1	9	3	7	1897.8960	3	5	11	6	5	2042.1115	2	−21
6	2	5	1834.6607	1	0	9	3	6	1897.9641	6	7	11	7	5	2093.2538	2	4
6	2	4	1834.9503		1	9	4	6	1925.4252	5	5	11	7	4	2093.2538	2	4
6	3	4	1854.4430	2	2	9	4	5	1925.4263	3	13	11	8	4	2151.7648	1	−3
6	3	3	1854.4491	4	0	9	5	5	1960.8552	2	0	11	8	3	2151.7648	1	−3
6	4	3	1882.0171	1	1	9	5	4	1960.8552	2	0	11	9	3	2219.8114	3	−5
6	4	2	1882.0171	1	1	9	6	4	2004.1842	2	−2	11	9	2	2219.8114	3	−5
6	5	2	1917.4894	2	0	9	6	3	2004.1842	2	−2	11	10	2	2294.5595	5	−14
6	5	1	1917.4894	2	0	9	7	3	2055.3867	1	0	11	10	1	2294.5595	5	−14
6	6	1	1960.8605	1	0	9	7	2	2055.3867	1	0	11	11	1	2377.2059	2	11
6	6	0	1960.8605	1	0	9	8	2	2114.1682	2	0	11	11	0	2377.2059	2	11
7	0	7	1831.0576	3	−2	9	8	1	2114.1682	2	0	12	0	12	1918.3282	1	1
7	1	7	1833.3209		−3	9	9	1	2181.7242	2	0	12	1	12	1919.1509		2

12	1	11	1930.3859	3	−6	14	1	13	1980.0281	1	−1	15	13	2	2663.5263	2	6
12	2	11	1936.9741	2	1	14	2	13	1985.1740	3	−1	15	14	2	2769.6213	1	0
12	2	10	1940.4907	4	5	14	2	12	1990.9544	3	−1	15	14	1	2769.6213	1	0
12	3	10	1957.7060	2	7	14	3	12	2006.6554	4	2	16	0	16	2017.7962	–	2
12	3	9	1958.0641	7	4	14	3	11	2007.5103	3	4	16	1	16	2018.0783	6	4
12	4	9	1985.1889	2	1	14	4	11	2034.1481	1	−2	16	1	15	2036.5297	3	−1
12	4	8	1985.2030	10	−16	14	6	8	2112.5945	5	9	16	2	15	2040.3164	2	3
12	5	8	2020.5362	5	−6	14	7	8	2163.6351	3	8	16	2	14	2048.9639	2	−8
12	5	7	2020.5362	5	−2	14	7	7	2163.6351	3	8	16	3	14	2062.8364	3	2
12	7	6	2114.9020	5	6	14	8	7	2221.8289	2	2	16	3	13	2064.6054	4	13
12	7	5	2114.9020	5	6	14	8	6	2221.8289	2	2	16	4	13	2090.4183	2	0
12	8	5	2173.2996	2	0	14	9	6	2290.5769	4	6	16	7	10	2219.6274	2	−2
12	8	4	2173.2996	2	0	14	9	5	2290.5769	4	6	16	7	9	2219.6274	2	−2
12	9	4	2241.5808	1	0	14	10	5	2365.4696	5	−3	16	8	9	2277.6319	2	1
12	9	3	2241.5808	1	0	14	10	4	2365.4696	5	−3	16	8	8	2277.6319	2	0
12	10	3	2316.3198	2	−5	14	11	4	2447.6879	2	2	16	9	8	2346.8596	2	3
12	10	2	2316.3198	2	−5	14	11	3	2447.6879	2	2	16	9	7	2346.8596	2	3
12	11	2	2398.8901	2	7	14	12	3	2538.1555	1	0	16	10	7	2422.1963	3	−8
12	11	1	2398.8901	2	7	14	12	2	2538.1555	1	0	16	10	6	2422.1963	3	−8
12	12	1	2489.4080	3	−1	14	13	2	2636.4659	1	0	16	11	6	2503.7294	3	−1
12	12	0	2489.4080	3	−1	14	13	1	2636.4659	1	0	16	11	5	2503.7294	3	−1
13	0	13	1940.7351	1	4	14	14	1	2742.5836	2	5	16	12	5	2594.1322	3	−2
13	1	13	1941.3751	2	6	14	14	0	2742.5836	2	5	16	12	4	2594.1322	3	−2
13	1	12	1954.3371	4	−6	15	0	15	1990.4682	–	4	16	13	4	2692.3922	2	6
13	2	12	1960.2020	2	0	15	1	15	1990.8425	–	7	16	13	3	2692.3922	2	6
13	2	11	1964.7722	2	1	15	1	14	2007.4330	3	−5	16	14	3	2798.4627	4	0
13	3	11	1981.2747	3	5	15	2	14	2011.8819	3	3	16	14	2	2798.4627	4	0
13	3	10	1981.8396	–	9	15	2	13	2019.0246	11	5	17	0	17	2046.7667	–	−7
13	4	10	2008.7555	1	0	15	3	13	2033.8444	2	1	17	1	17	2046.9782	1	−1
13	5	9	2044.0643	6	−7	15	3	12	2035.0927	9	−6	17	1	16	2067.2951	1	0
13	5	8	2044.0637	7	−4	15	4	12	2061.3686	2	−4	17	2	16	2070.4694	2	2
13	7	7	2138.3618	4	8	15	5	11	2096.5906	4	25	17	2	15	2080.7566	2	−8
13	7	6	2138.3618	4	8	15	5	10	2096.5817	5	−15	17	3	15	2093.6245	2	0
13	8	6	2196.6546	1	0	15	6	9	2139.7202	5	−26	17	3	14	2096.0538	1	−1
13	8	5	2196.6546	1	0	15	7	9	2190.7228	2	2	17	4	14	2121.2963	–	0
13	9	5	2265.1687	3	2	15	7	8	2190.7228	2	2	17	7	11	2250.3495	8	−7
13	9	4	2265.1687	3	2	15	8	8	2248.8214	1	1	17	7	10	2250.3495	8	−6
13	10	4	2339.9467	2	9	15	8	7	2248.8214	1	1	17	8	10	2308.2603	2	1
13	10	3	2339.9467	2	9	15	9	7	2317.8067	3	6	17	8	9	2308.2603	2	1
13	11	3	2422.3840	3	5	15	9	6	2317.8067	3	6	17	9	9	2377.7375	1	0
13	11	2	2422.3840	3	5	15	10	6	2392.8921	2	2	17	9	8	2377.7375	1	0
13	12	2	2512.8782	2	0	15	10	5	2392.8921	2	2	17	10	8	2453.3823	2	3
13	12	1	2512.8782	2	0	15	11	5	2474.8027	2	0	17	10	7	2453.3823	2	3
13	13	1	2611.2106	3	−9	15	11	4	2474.8027	2	0	17	11	7	2534.4692	1	0
13	13	0	2611.2106	3	−9	15	12	4	2565.2399	2	−2	17	11	6	2534.4692	1	0
14	0	14	1964.7816	–	5	15	12	3	2565.2399	2	−2	17	12	6	2624.8324	2	−2
14	1	14	1965.2743	–	15	15	13	3	2663.5263	2	6	17	12	5	2624.8324	2	−2
17	13	5	2723.0639	4	5	19	14	6	2895.8083	1	1	22	12	10	2805.4741	1	1
17	13	4	2723.0639	4	5	19	14	5	2895.8083	1	1	22	13	10	2903.5162	2	2
17	14	4	2829.1072	2	−1	20	0	20	2143.5542	19	−1	22	13	9	2903.5162	2	2
17	14	3	2829.1072	2	−1	20	1	20	2143.6395	5	0	22	14	9	3009.3928	2	−1
18	0	18	2077.3830	6	−5	20	1	19	2169.4435	3	9	22	14	8	3009.3928	2	−1

Table 4 (*continued*)

J	K_a 1	K_c	E 2	Δ 3	δ 4	J	K_a 1	K_c	E 2	Δ 3	δ 4	J	K_a 1	K_c	E 2	Δ 3	δ 4
18	1	18	2077.5395	5	−8	20	2	19	2171.1573	4	−5	23	2	22	2287.0354	12	−4
18	1	17	2099.7114	2	4	20	2	18	2187.0306	5	10	23	9	15	2601.4394	6	8
18	2	17	2102.3325	1	1	20	3	18	2196.6930	14	−1	23	9	14	2601.4394	6	1
18	2	16	2114.3810	6	−6	20	3	17	2202.0883	2	−3	23	11	13	2757.1025	4	2
18	3	16	2126.2026	9	2	20	8	13	2411.0560	4	6	23	11	12	2757.1025	4	2
18	3	15	2129.4501	4	−8	20	8	12	2411.0560	4	−8	23	12	12	2847.0351	1	0
18	7	12	2282.8911	3	0	20	9	12	2481.3403	2	−1	23	12	11	2847.0351	1	0
18	7	11	2282.8911	3	1	20	9	11	2481.3403	2	−2	23	13	11	2945.0280	2	6
18	8	11	2340.7067	2	0	20	11	10	2637.5835	2	3	23	13	10	2945.0280	2	6
18	8	10	2340.7067	2	−1	20	11	9	2637.5835	2	3	23	14	10	3050.8638	2	−3
18	9	10	2410.4423	2	−2	20	12	9	2727.7870	2	0	23	14	9	3050.8638	2	−3
18	9	9	2410.4423	2	−2	20	12	8	2727.7870	2	0	24	2	23	2329.0068	2	−1
18	11	8	2567.0234	1	0	20	13	8	2825.9155	5	0	24	9	16	2645.1482	3	1
18	11	7	2567.0234	1	0	20	13	7	2825.9155	5	0	24	9	15	2645.1485	3	−2
18	12	7	2657.3414	2	−2	20	14	7	2931.8650	3	0	24	11	14	2800.6147	1	0
18	12	6	2657.3414	2	−2	20	14	6	2931.8650	3	0	24	11	13	2800.6147	1	0
18	13	6	2755.5413	2	0	21	0	21	2179.1084	3	−10	24	12	13	2890.4091	1	0
18	13	5	2755.5413	2	0	21	1	21	2179.1744	–	26	24	12	12	2890.4091	1	0
18	14	5	2861.5557	1	0	21	1	20	2206.7441	3	15	24	13	12	2988.3478	–	−3
18	14	4	2861.5557	1	0	21	2	20	2208.1039	–	−13	24	13	11	2988.3478	–	−3
19	0	19	2109.6433	–	−24	21	9	13	2519.5376	2	1	24	14	11	3094.1397	2	1
19	1	19	2109.7603	–	−13	21	9	12	2519.5376	2	0	24	14	10	3094.1397	2	1
19	1	18	2133.7641	2	7	21	11	11	2675.5946	1	1	25	11	15	2845.9875	1	1
19	2	18	2135.8979	3	2	21	11	10	2675.5946	1	1	25	11	14	2845.9875	1	1
19	2	17	2149.8138	2	−2	21	12	10	2765.7251	1	1	25	12	14	2935.5969	3	−7
19	3	17	2160.5619	3	2	21	12	9	2765.7251	1	1	25	12	13	2935.5969	3	−7
19	3	16	2164.7958	5	−12	21	13	9	2863.8120	3	−2	25	13	13	3033.4759	2	−3
19	8	12	2374.9719	2	4	21	13	8	2863.8120	3	−2	25	13	12	3033.4759	2	−3
19	8	11	2374.9719	2	−1	21	14	8	2969.7266	1	0	25	14	12	3139.2213	3	−2
19	9	11	2444.9759	2	−3	21	14	7	2969.7266	1	0	25	14	11	3139.2213	3	−2
19	9	10	2444.9759	2	−3	22	0	22	2216.3118	15	14	26	12	15	2982.5993	5	6
19	11	9	2601.3939	3	0	22	2	21	2246.7329	12	−4	26	12	14	2982.5993	5	6
19	11	8	2601.3939	3	0	22	9	14	2559.5697	2	2	26	14	13	3186.1082	1	0
19	12	8	2691.6594	2	−1	22	9	13	2559.5697	2	−1	26	14	12	3186.1082	1	0
19	12	7	2691.6594	2	−1	22	11	12	2715.4324	2	−1	27	12	16	3031.4191	2	−1
19	13	7	2789.8251	2	−2	22	11	11	2715.4324	2	−1	27	12	15	3031.4191	2	−1
19	13	6	2789.8251	2	−2	22	12	11	2805.4741	1	1						

[a] Δ is the experimental uncertainty in the upper energy value in units of 10^{-4} cm^{-1} (Δ is absent when the upper energy value was determined from a single transition); δ is the difference $E^{exp.} - E^{calc.}$ also in units of 10^{-4} cm^{-1}.

Table 5
Ro-vibrational term values for the ($v_{10} = v_{12} = 1$) vibrational state of the C_2H_4 molecule (in cm^{-1})[a].

J	K_a 1	K_c	E 2	Δ 3	δ 4	J	K_a 1	K_c	E 2	Δ 3	δ 4	J	K_a 1	K_c	E 2	Δ 3	δ 4
1	0	1	2266.7793		1	7	4	4	2377.4391	4	−3	10	5	5	2461.1934	2	−2
1	1	1	2270.5440		0	7	4	3	2377.4391	4	−6	10	6	5	2503.5350	4	−6
1	1	0	2270.7087	2	1	7	5	3	2412.0804	5	0	10	6	4	2503.5350	4	−6
2	0	2	2270.4053		3	7	5	2	2412.0804	5	0	10	7	4	2553.6195	4	3
2	1	2	2274.0104	1	−1	7	6	2	2454.4506		3	10	7	3	2553.6195	4	3
2	1	1	2274.5048	2	5	7	6	1	2454.4506		3	10	8	3	2611.4416	2	5
2	2	0	2285.8055	4	−1	7	7	1	2504.5522	2	10	10	8	2	2611.4416	2	5
3	0	3	2275.8310	3	4	7	7	0	2504.5522	2	10	10	9	2	2676.9992	5	−3
3	1	3	2279.2067	2	−2	8	0	8	2329.2704	1	0	10	9	1	2676.9992	5	−3
3	1	2	2280.1948	6	5	8	1	8	2330.9676	2	−7	11	0	11	2381.5684	2	3
3	2	1	2291.2735		1	8	1	7	2336.8517	3	0	11	2	9	2402.8031		9
3	3	1	2310.4937	2	2	8	2	6	2346.6111	3	6	11	3	9	2419.7926	10	12
3	3	0	2310.4937	2	1	8	3	6	2365.0973	3	4	11	4	8	2446.6526	13	5
4	0	4	2283.0400	2	−1	8	3	5	2365.1455	1	0	11	4	7	2446.6638	6	4
4	1	4	2286.1287	3	−7	8	4	5	2391.9987	8	5	11	5	7	2481.2160	4	3
4	1	3	2287.7759	2	7	8	4	4	2391.9987	8	−4	11	5	6	2481.2160	4	1
4	2	2	2298.5845	5	5	8	5	4	2426.6279	6	2	11	6	6	2523.5411	1	0
4	3	2	2317.7663	2	4	8	5	3	2426.6279	6	2	11	6	5	2523.5411	1	0
4	3	1	2317.7663	2	−3	8	6	3	2468.9912	2	−1	11	7	5	2573.6144	3	−1
4	4	1	2344.7066	3	2	8	6	2	2468.9912	2	−1	11	7	4	2573.6144	3	−1
4	4	0	2344.7066	3	2	8	7	2	2519.0883	2	1	11	8	4	2631.4293	2	−3
5	0	5	2292.0134		2	8	7	1	2519.0883	2	1	11	8	3	2631.4293	2	−3
5	1	5	2294.7720		−8	8	8	1	2576.9204		6	11	9	3	2696.9833		4
5	1	4	2297.2408	3	7	8	8	0	2576.9204		6	11	9	2	2696.9833		4
5	2	3	2307.7541		3	9	0	9	2345.0552	4	−2	12	0	12	2402.2790		3
5	3	3	2326.8610		6	9	1	9	2346.4326	2	−4	12	1	12	2402.9344	3	5
5	3	2	2326.8632	2	0	9	1	8	2353.7510	2	−17	12	2	10	2425.4053	2	9
5	4	2	2353.7952	4	−3	9	2	7	2363.4026	2	0	12	3	10	2441.6818	4	1
5	4	1	2353.7952	4	−3	9	3	7	2381.4962		−27	12	4	9	2468.5380	1	0
5	5	1	2388.4494	2	3	9	3	6	2381.5952	4	−4	12	4	8	2468.5606	4	1
5	5	0	2388.4494	2	3	9	4	6	2408.3859	18	10	12	5	8	2503.0674	5	6
6	0	6	2302.7258	3	−4	9	4	5	2408.3859	18	−12	12	5	7	2503.0674	5	1
6	1	6	2305.1305	5	−9	9	5	5	2442.9981	5	−1	12	6	7	2545.3712	3	2
6	1	5	2308.5827	5	11	9	5	4	2442.9981	5	−1	12	6	6	2545.3712	3	2
6	2	4	2318.8024		5	9	6	4	2485.3521	3	−7	12	7	6	2595.4310	1	0
6	3	4	2337.7790	6	0	9	6	3	2485.3521	3	−7	12	7	5	2595.4310	1	0
6	3	3	2337.7878	5	−1	9	7	3	2535.4439	3	0	12	8	5	2653.2365	2	−7
6	4	3	2364.7056	3	−2	9	7	2	2535.4439	3	0	12	8	4	2653.2365	2	−7
6	4	2	2364.7056	3	−3	9	8	2	2593.2723	6	10	12	9	4	2718.7842	3	2
6	5	2	2399.3543	6	−3	9	8	1	2593.2723	6	10	12	9	3	2718.7842	3	2
6	5	1	2399.3543	6	−3	10	0	10	2362.4919	1	2	13	0	13	2424.6210	1	−2
7	1	7	2317.1978	6	−10	10	2	8	2382.1340	1	0	13	2	11	2449.9297	2	5
7	1	6	2321.7897		1	10	3	8	2399.7315	6	9	13	3	11	2465.3951		23
7	2	5	2331.7486		5	10	4	7	2426.6019		0	13	4	10	2492.2631	5	2
7	3	5	2350.5245	4	6	10	4	6	2426.6067	10	−5	13	4	9	2492.3043	1	−5
7	3	4	2350.5460	2	−1	10	5	6	2461.1934	2	−1	13	5	9	2526.7504	6	9
13	5	8	2526.7504	6	−2	14	5	9	2552.2688		3	15	9	6	2795.0962	3	8
13	6	8	2569.0272	5	4	14	7	8	2644.5328	3	7	16	0	16	2501.4454		−16
13	6	7	2569.0272	5	5	14	7	7	2644.5328	3	7	16	1	16	2501.6476	3	−4
13	7	7	2619.0701	2	3	14	8	7	2702.3121	2	−4	16	5	12	2608.8141	4	−4
13	7	6	2619.0701	2	3	14	8	6	2702.3121	2	−5	16	9	8	2824.1714	2	1
13	8	6	2676.8641	3	−5	14	9	6	2767.8404	6	6	16	9	7	2824.1714	2	1
13	8	5	2676.8641	3	−5	14	9	5	2767.8404	6	6	17	1	17	2530.4726		10
13	9	5	2742.4028	2	0	15	1	15	2474.4778	2	−6	17	5	12	2639.8639	1	0
13	9	4	2742.4028	2	−1	15	4	11	2545.3633		−20	17	9	9	2855.0668		−10
14	0	14	2448.5955		−6	15	5	11	2579.6184		−21	17	9	8	2855.0668		−10
14	1	14	2448.9666	1	−1	15	5	10	2579.6255	6	9	18	9	10	2887.7823	3	0
14	2	12	2476.3617		−1	15	7	9	2671.8203		6	18	9	9	2887.7823	3	0
14	3	12	2490.9280	4	1	15	7	8	2671.8203		6	18	5	14	2672.7258	1	−1
14	4	11	2517.8283	5	−6	15	8	8	2729.5825	5	7	18	5	13	2672.7551	2	2
14	4	10	2517.9027		−8	15	8	7	2729.5825	5	6	20	1	20	2626.8047		0
14	5	10	2552.2668		3	15	9	7	2795.0962	3	8						

[a] Δ is the experimental uncertainty in the upper energy value in units of 10^{-4} cm^{-1} (Δ is absent when the upper energy value was determined from a single transition); δ is the difference $E^{exp.} - E^{calc.}$ also in units of 10^{-4} cm^{-1}.

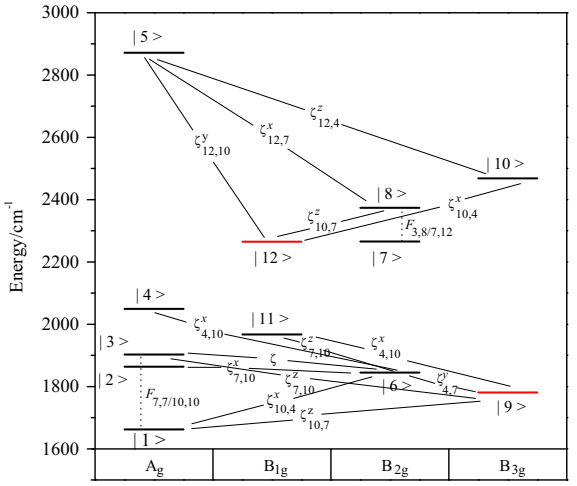

Fig. 6. The g-type vibrational levels of C_2H_4 in the region 1600–2900 cm^{-1}. Resonance interaction between different vibrational states are shown: "F" denotes interactions between the states of the same symmetry; "ζ_{ij}^{α}" ($\alpha = x, y, z$) denote Coriolis-type interactions.

$$+{}^{v\tilde{v}}C^{i}_{KKK}J_z^6+{}^{v\tilde{v}}C^{i}_{KKJ}J_z^4J^2+{}^{v\tilde{v}}C^{i}_{KJJ}J_z^2J^4$$
$$+\frac{1}{2}{}^{v\tilde{v}}C^{i}_{JJJ}J^6+\cdots \qquad (8)$$

To prevent confusion in the label notations used, we should mention that we use two sets of axis notation in the C_2H_4 molecule. Firstly, the x-, y- and z-axes are used for labeling of rotational operators J_α ($\alpha = x, y$ or z). However, for the point group symmetry assignment of normal modes we use the standard convention in accordance with Ref. [39].

4. Description of the spectrum and assignments of transitions

The reader can see the survey spectra in the regions of location of the $\nu_7+\nu_{10}-\nu_{10}$ and $\nu_{10}+\nu_{12}-\nu_{10}$ bands on Figs. 1 and 2, respectively. The main part of absorbance in these regions is caused by the strong fundamental bands ν_7 and ν_{12}. The "hot" bands $\nu_7+\nu_{10}-\nu_{10}$ and $\nu_{10}+\nu_{12}-\nu_{10}$ are considerably weaker: the ratio of intensity of the "hot" band to intensity of the corresponding "cold" band is about 0.020. "Black" and "grey" spectra on Figs. 1 and 2 correspond to different sample pressures during recording (0.1 and 50.0 Pa in the region 800–1130 cm^{-1}, and 13 and 200 Pa in the region 1360–1540 cm^{-1}). Centers of both the "cold", and "hot" bands are marked in Figs. 1 and 2. Figs. 4 and 5 show small fragments of spectra in both spectral regions: transitions belonging the "hot" bands are marked by dark triangles.

Because the $\nu_7+\nu_{10}-\nu_{10}$ is the c-type band, transitions are allowed which satisfy the selection rules

$$\Delta J = 0, \pm 1, \quad \Delta K_a = odd, \quad \Delta K_c = even. \qquad (9)$$

In this case, transitions with $\Delta K_a = \pm 1$, and $\Delta K_c = 0$ are the "allowed" ones, and they are considerably stronger than "forbidden" transitions which correspond the general rules, Eq. (9). Analogously, the $\nu_{10}+\nu_{12}-\nu_{10}$ is the a-type band, and selection rules for it are

$$\Delta J = 0, \pm 1, \quad \Delta K_a = even, \quad \Delta K_c = odd. \qquad (10)$$

Again "allowed" transitions ($\Delta K_a = 0$, and $\Delta K_c = \pm 1$) are considerably stronger than "forbidden" ones.

For assignment of transitions we used the traditional combination differences method. In this case, the values of ro-vibrational energies of the lower vibrational state, ($v_{10} = 1$), have been calculated with the parameters from Ref. [40]. As a result of assignment, about 930 and 370 transitions with the maximum values of upper quantum numbers, $J^{max.}/K_a^{max.}$, equal to 27/14 and 20/9 have been assigned to the $\nu_7+\nu_{10}-\nu_{10}$ and $\nu_{10}+\nu_{12}-\nu_{10}$ bands, respectively (for more details, see statistical information in Table 2). The complete list of assigned transitions is presented in the Supplementary Materials (for illustration, a small part of this list is shown in Table 3). Because the studied bands are weak and, as a rule, their lines are covered by the considerably stronger lines of the bands ν_7 and ν_{12}, the experimental accuracy in line positions of the $\nu_7+\nu_{10}-\nu_{10}$ and $\nu_{10}+\nu_{12}-\nu_{10}$ bands are worse than accuracy of lines belonging to the ν_7 and ν_{12} bands. In general, accuracy in positions of "hot" transitions in our experiment was estimated as $(3-6)\times 10^{-4}$ cm^{-1}. The assigned transitions were used then for determination of ro-vibrational energies of the g-type vibrational states ($v_7 = v_{10} = 1, B_{3g}$) and ($v_{10} = v_{12} = 1, B_{1g}$). Corresponding energy values (404 for the ($v_7 = v_{10} = 1$) vibrational state, and 185 for the ($v_{10} = v_{12} = 1$) one) are presented in columns 2 of Tables 4 and 5 together with values Δ in columns 3 (Δ is the experimental uncertainty in the upper energy value in units of 10^{-4} cm^{-1}; Δ is absent when the upper energy value was determined from a single transition).

5. Ro-vibrational analysis of the states ($v_7 = v_{10} = 1$) and ($v_{10} = v_{12} = 1$)

The 589 upper ro-vibrational energies obtained from the analysis of experimental data were used then in the fit procedure with the hamiltonian model from Section 3. As was discussed above, to provide a correct analysis, we used a model which takes into account 12 interacting vibrational states (see Fig. 6). From these 12 vibrational states, energies of only two of them have been obtained from our analysis of experimental data. So, 10 others should be considered as "dark" states. In this case, the most important point is how to estimate more or less correct values of both parameters of the "dark" states, and parameters of the resonance interactions between the considered states. In our case we used the following procedure:

(1) The initial values of unperturbed vibrational energies (parameters E^v in Eq. (3)), with the exception of vibrational energy of the ($v_{10} = 2$) state, have been estimated on the basis of the values of harmonic frequencies, ω_λ, and anharmonic coefficients, $x_{\lambda\mu}$ ($\lambda, \mu = 1, 2, \ldots, 12$) from Ref. [17].
(2) The value $E^{(v_{10}=2)}$ was taken as 1662.2 cm^{-1}, Ref. [21].
(3) The other parameters of the doubly excited vibrational states (diagonal blocks, H^{vv}, in Eq. (2)), with the exception

Table 6
Spectroscopic parameters of the lowest "g"-type vibrational states of the C_2H_4 molecule (in cm^{-1})[a].

Parameter	Ground	|1⟩	|9⟩	|6⟩	|2⟩	|3⟩	|11⟩
1	2	3	4	5	6	7	8
E	1662.20(686)	1781.007803(207)	1844.794(105)	1863.72(170)	1902.44322(605)	1902.44322(605)	967.244
A	4.86461997815	4.93604(559)	4.8373873(244)	4.93298(207)	4.83951344(204)	4.890759(173)	4.850580572
B	1.00105650691	1.06675(514)	0.99448872(762)	0.96392(159)	1.00679487(212)	1.030674(756)	0.9966357431
C	0.82804595595	0.81012(475)	0.8291538(529)	0.8264222961	0.82462858(166)	0.8306368841	0.8293689141
$\Delta_K \times 10^4$	0.86470155	0.90751305	0.8861073	0.8861073	0.86470155	0.86470155	0.86470155
$\Delta_{JK} \times 10^4$	0.102336194	0.102336194	0.1028003	0.0987461	0.102336194	0.1032644	0.099210206
$\Delta_J \times 10^4$	0.014701077	0.014701077	0.01475178	0.014701077	0.014701077	0.014802483	0.014751773
$\delta_K \times 10^4$	0.10153495	0.10572645	0.0996140	0.10388715	0.10153495	0.09350155	0.09777470
$\delta_J \times 10^4$	0.0028179017	0.0028179017	0.0028075083	0.0028179017	0.0028179017	0.0027971183	0.0028075083
$H_K \times 10^8$	0.621279	0.621279	0.64669	0.621279	0.621279	0.672101	0.64669
$H_{KJ} \times 10^8$	−0.041497	−0.041497	−0.041497	−0.041497	−0.041497	−0.041497	−0.041497
$H_{JK} \times 10^8$	0.018693	0.018693	0.014952	0.018693	0.018693	0.011211	0.014952
$H_J \times 10^8$	0.00023588	0.00023588	0.00021640	0.00023588	0.00023588	0.00019692	0.00021640
$h_K \times 10^8$	0.34059	0.34059	0.34059	0.34059	0.34059	0.34059	0.34059
$h_{JK} \times 10^8$	0.0103566	0.0103566	0.0103566	0.0103566	0.0103566	0.0103566	0.0103566
$h_J \times 10^8$	0.000125178	0.000125178	0.000125178	0.000125178	0.000125178	0.000125178	0.000125178
$L_K \times 10^{12}$	−0.4467	−0.4467	−0.4467	−0.4467	−0.4467	−0.4467	−0.4467
$L_{JK} \times 10^{12}$	−0.004492	−0.004492	−0.004492	−0.004492	−0.004492	−0.004492	−0.004492
$L_J \times 10^{12}$	−0.0000172	−0.0000172	−0.0000172	−0.0000172	−0.0000172	−0.0000172	−0.0000172

Parameter	|4⟩	|12⟩	|7⟩	|8⟩	|10⟩	|5⟩
1	9	10	11	12	13	14
E	2049.595	2264.963530(240)	2265.93(120)	2374.09(183)	2468.072	2871.627
A	4.827820022	4.9310294(397)	4.864619978	4.856427282	4.833666732	4.83951344
B	0.9965749731	1.0056714(101)	1.001056507	0.99232(118)	1.001684923	1.00679487
C	0.8281009441	0.8251654(105)	0.82804595595	0.827632734	0.826364764	0.82462858
$\Delta_K \times 10^4$	0.86470155	0.88805475	0.86470155	0.8666490	0.8666490	0.86470155
$\Delta_{JK} \times 10^4$	0.095156006	0.1116283	0.102336194	0.112092406	0.108038206	0.102336194
$\Delta_J \times 10^4$	0.014701063	0.01474409	0.014701077	0.014794793	0.014744083	0.014701077
$\delta_K \times 10^4$	0.10204785	0.10693725	0.10153495	0.1008248	0.10509795	0.10153495
$\delta_J \times 10^4$	0.0028178983	0.00289684	0.0028179017	0.0028864483	0.0028968383	0.0028179017
$H_K \times 10^8$	0.621279	0.621279	0.621279	0.64669	0.621279	0.621279
$H_{KJ} \times 10^8$	−0.041497	−0.041497	−0.041497	−0.041497	−0.041497	−0.041497
$H_{JK} \times 10^8$	0.018693	0.018693	0.018693	0.014952	0.018693	0.018693
$H_J \times 10^8$	0.00023588	0.00023588	0.00023588	0.0002164	0.00023588	0.00023588
$h_K \times 10^8$	0.34059	0.34059	0.34059	0.34059	0.34059	0.34059
$h_{JK} \times 10^8$	0.0103566	0.0103566	0.0103566	0.0103566	0.0103566	0.0103566
$h_J \times 10^8$	0.000125162	0.000125178	0.000125178	0.000125178	0.000125178	0.000125178
$L_K \times 10^{12}$	−0.4467	−0.4467	−0.4467	−0.4467	−0.4467	−0.4467
$L_{JK} \times 10^{12}$	−0.004492	−0.004492	−0.004492	−0.004492	−0.004492	−0.004492
$L_J \times 10^{12}$	−0.0000172	−0.0000172	−0.0000172	−0.0000172	−0.0000172	−0.0000172

[a] Values in parentheses are 1σ standard errors. Values of parameters presented without standard errors have been estimated theoretically (see text for details) and were not varied in the fit procedure.

of parameters of the states $(v_8 = 2)$ and $(v_3 = v_8 = 1)$, have been estimated in accordance with a simple formula

$$P^{(v_\lambda = v_\mu = 1)} = P^{(v_\lambda = 1)} + P^{(v_\mu = 1)} - P^{(gr.)}, \quad (11)$$

where $P^{(v_1,\ldots,v_{12})}$ is any of the rotational, A, B, C, or centrifugal distortion, Δ_K, Δ_{JK}, Δ_J, etc., parameters of the $(v_1,\ldots,v_{12})$ or the ground vibrational state; $\lambda,\mu = 1,\ldots,12$. The values of initial parameters in the right hand site of Eq. (11) have been taken from Ref. [40].

(4) Values of rotational and centrifugal distortion parameters of the $(v_8 = 2)$ and $(v_3 = v_8 = 1)$ states have been constrained to the values of corresponding parameters of the ground vibrational state from Ref. [40].

(5). The main Coriolis interaction parameters ${}^{\nu\tilde{\nu}}C^i$, $i = 1, 2$ (see Eqs. (5)–(8)) can be estimated as

$${}^{(v_\lambda = v_\mu = 1),(v_\lambda = v_\nu = 1)}C^i = {}^{(v_\mu = 1),(v_\nu = 1)}C^i, \quad (12)$$

or

$$\begin{aligned} {}^{(v_\lambda = 2),(v_\lambda = v_\mu = 1)}C^i &= -{}^{(v_\lambda = v_\mu = 1),(v_\lambda = 2)}C^i \\ &= \sqrt{2}\,{}^{(v_\lambda = 1),(v_\mu = 1)}C^i. \end{aligned} \quad (13)$$

Here λ, μ, and ν are all different. The values of initial parameters in the right hand side of Eqs. (12) and (13) also have been taken from Ref. [40] (in particular, the initial values for the main ${}^{\cdots}C^{\cdots}$ parameters have been

Table 7
Coriolis interaction parameters for the lowest "g"-type vibrational states of the C_2H_4 molecule (in cm^{-1})[a].

Parameter	Value	Parameter	Value	Parameter	Value
$(2B\zeta^x)^{1,6}$	2.501297734	${}^{1,6}C^1_K \times 10^2$	1.9014(177)	${}^{1,6}C^1_J \times 10^3$	−1.3776(417)
${}^{1,6}C^1_{KK} \times 10^4$	−2.2261(247)	${}^{1,6}C^1_{KJ} \times 10^5$	1.1215(467)	${}^{1,6}C^1_{JJ} \times 10^7$	−4.979(611)
${}^{1,6}C^1_{KKK} \times 10^7$	5.5753(979)	${}^{1,6}C^1_{KKJ} \times 10^8$	−2.741(179)	${}^{1,6}C^2 \times 10^4$	−9.3205159
${}^{1,6}C^2_K \times 10^3$	−1.5365(296)	${}^{1,6}C^2_{KK} \times 10^6$	5.370(238)	${}^{1,6}C^2_{KJ} \times 10^7$	−1.6217(974)
${}^{1,6}C^2_{KKK} \times 10^9$	2.947(391)	${}^{1,6}C^3_K \times 10^6$	−4.854(186)	${}^{1,6}C^3_J \times 10^7$	6.191(422)
${}^{2,6}C^1_J \times 10^4$	4.978(348)	${}^{2,6}C^2_J \times 10^5$	−1.266(152)	${}^{2,6}C^3 \times 10^4$	−5.667(203)
${}^{3,6}C^1_K \times 10^3$	5.374(150)	${}^{3,6}C^2 \times 10^2$	−4.041	${}^{3,6}C^2_K \times 10^4$	9.507(160)
${}^{3,6}C^2_{KK} \times 10^6$	−3.022(138)				
$(2B\zeta^x)^{4,6}$	−2.501297734	${}^{4,6}C^2 \times 10^4$	−9.320515902		
$(2B\zeta^x)^{5,8}$	1.89817112	${}^{5,8}C^2 \times 10^2$	2.0787553		
$(2A\zeta^z)^{5,10}$	7.7970919				
$(2B\zeta^x)^{9,11}$	1.76868459	${}^{9,11}C^2 \times 10^3$	−6.59060		
$(2B\zeta^x)^{10,12}$	−1.76868459	${}^{10,12}C^2 \times 10^3$	−6.59060		
$(2C\zeta^y)^{6,9}$	−0.22082(527)	${}^{6,9}C^1_K \times 10^4$	−7.16(106)	${}^{6,9}C^1_J \times 10^4$	−3.3039(303)
${}^{6,9}C^1_{KK} \times 10^5$	−5.873(116)	${}^{6,9}C^1_{JJ} \times 10^7$	2.9752(876)	${}^{6,9}C^1_{KKK} \times 10^7$	4.0541(676)
${}^{6,9}C^1_{JJJ} \times 10^{10}$	−3.784(624)	${}^{6,9}C^2 \times 10^2$	1.1212(634)	${}^{6,9}C^2_K \times 10^4$	6.9437(824)
${}^{6,9}C^2_J \times 10^5$	−6.8277(977)	${}^{6,9}C^2_{KK} \times 10^6$	−6.0972(642)	${}^{6,9}C^2_{JJ} \times 10^8$	6.663(105)
${}^{6,9}C^2_{KKK} \times 10^8$	1.5221(254)	${}^{6,9}C^3 \times 10^5$	−5.86(102)		
$(2C\zeta^y)^{5,12}$	−0.202641	${}^{5,12}C^2 \times 10^2$	−1.4958		
$(2A\zeta^z)^{1,9}$	−6.198429876	${}^{1,9}C^1_J \times 10^3$	5.4698(105)	${}^{1,9}C^1_{JJ} \times 10^6$	−3.3805(319)
${}^{1,9}C^2 \times 10^4$	−6.149141989	${}^{1,9}C^2_J \times 10^5$	2.0128(297)	${}^{1,9}C^3 \times 10^3$	1.6492(149)
${}^{1,9}C^3_K \times 10^6$	−2.557(117)	${}^{1,9}C^3_J \times 10^6$	−2.2896(398)		
$(2A\zeta^z)^{3,9}$	6.198429876	${}^{3,9}C^1_J \times 10^3$	−4.58391(893)	${}^{3,9}C^1_{JJ} \times 10^6$	1.3716(347)
${}^{3,9}C^1_{KJJ} \times 10^9$	3.6910(967)	${}^{3,9}C^2 \times 10^4$	−6.149141989	${}^{3,9}C^2_K \times 10^4$	−1.8633(226)
${}^{3,9}C^2_{KK} \times 10^6$	1.2979(297)	${}^{3,9}C^3_J \times 10^7$	4.7289(916)		
$(2A\zeta^z)^{6,11}$	−4.382951799	${}^{6,11}C^2 \times 10^4$	−4.3481		
$(2A\zeta^z)^{8,12}$	4.3829518	${}^{8,12}C^1_K \times 10^4$	−3.4509(713)	${}^{8,12}C^1_J \times 10^4$	−1.7409(527)
${}^{8,12}C^1_{KK} \times 10^7$	8.281(105)	${}^{8,12}C^2 \times 10^4$	−4.3481	${}^{8,12}C^2_K \times 10^4$	−3.776(319)
${}^{8,12}C^2_J \times 10^5$	−2.6165(543)	${}^{8,12}C^2_{KK} \times 10^6$	4.989(572)	${}^{8,12}C^2_{KJ} \times 10^8$	7.145(102)
${}^{8,12}C^2_{JJ} \times 10^7$	1.382(144)	${}^{8,12}C^2_{JJJ} \times 10^{10}$	−2.158(184)		

[a] Values in parentheses are 1σ standard errors. Values of parameters presented without standard errors have been estimated theoretically (see text for details) and were not varied in the fit procedure.

Table 8
Fermi interaction parameters for some lowest "g"-type vibrational states of the C_2H_4 molecule (in cm^{-1})[a].

Parameter	Value	Parameter	Value	Parameter	Value
${}^{1,3}F_K \times 10^2$	−1.6193(149)				
${}^{7,8}F_0 \times 10^2$	2.209(149)	${}^{7,8}F_K \times 10^3$	2.4873(379)	${}^{7,8}F_J \times 10^4$	−3.179(485)
${}^{7,8}F_{KK} \times 10^5$	2.178(585)				

[a] Values in parentheses are 1σ standard errors. Values of parameters presented without standard errors have been estimated theoretically (see text for details) and were not varied in the fit procedure.

taken as ${}^{(v_4=1),(v_7=1)}C^2 = 0.6689444 \times 10^{-2}\ cm^{-1}$, ${}^{(v_4=1),(v_{10}=1)}C^1 = (2B\zeta^x)^{4,10} = -1.76868459\ cm^{-1}$, ${}^{(v_4=1),(v_{10}=1)}C^2 = -0.65906 \times 10^{-2}\ cm^{-1}$, ${}^{(v_4=1),(v_{12}=1)}C^1 = (2A\zeta^z)^{4,12} = -5.5133766\ cm^{-1}$, ${}^{(v_4=1),(v_{12}=1)}C^2 = -0.65906 \times 10^{-2}\ cm^{-1}$, ${}^{(v_7=1),(v_{10}=1)}C^1 = (2A\zeta^z)^{7,10} = -4.382951799\ cm^{-1}$, ${}^{(v_7=1),(v_{10}=1)}C^2 = -0.43481 \times 10^{-3}\ cm^{-1}$, ${}^{(v_7=1),(v_{12}=1)}C^1 = (2B\zeta^x)^{7,12} = -1.34220967\ cm^{-1}$, ${}^{(v_7=1),(v_{12}=1)}C^2 = -0.01469902\ cm^{-1}$, ${}^{(v_{10}=1),(v_{12}=1)}C^1 = (2C\zeta^y)^{10,12} = 0.143289\ cm^{-1}$, ${}^{(v_{10}=1),(v_{12}=1)}C^2 = -1.0577 \times 10^{-2}\ cm^{-1}$). The estimated values of all the discussed parameters can be seen in Tables 6 and 7.

In the fit procedure we followed the strategy of our recent studies of sets of strongly interacting vibrational states of a

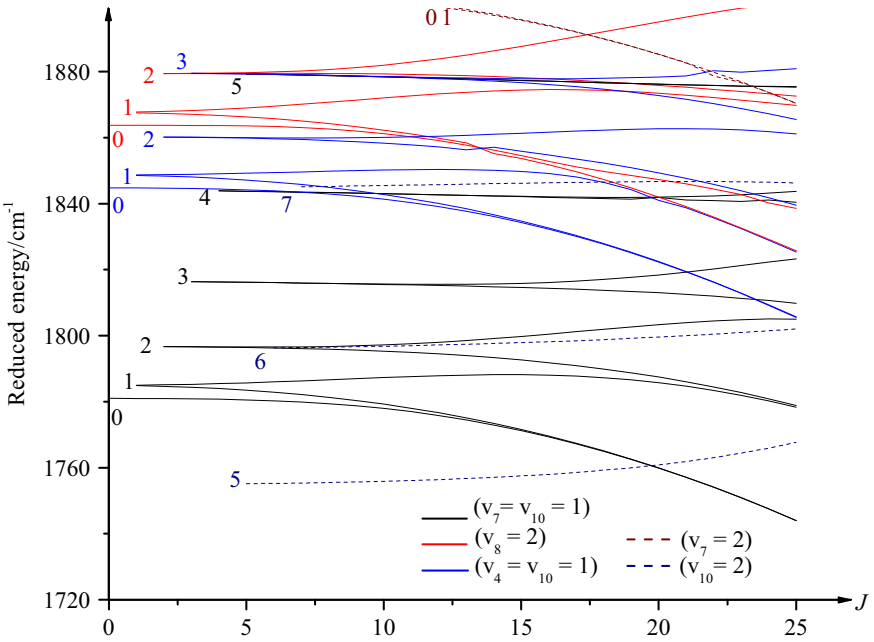

Fig. 7. Fragment of ro-vibrational energy levels of the lowest *g*-type vibrational states. The energies have been calculated from the constants given in Tables 6–8. In order to suppress most of the *J*-slope the calculated energies have been reduced by $((B+C)/2)J(J+1)$. Levels belonging to different vibrational states are marked by different colors. Numbers 1, 2, … indicated on the left part of Fig. 7 are quantum numbers K_a of ro-vibrational states. (For interpretation of the references to color in this figure caption, the reader is referred to the web version of this article.)

molecules (see, *e.g.*, Refs. [40–44], which correlates with the main statements of the general rotation–vibration theory, Ref. [45]. Namely, in accordance with the general rotation–vibration theory, the value of any physically suitable effective rotational or centrifugal distortion parameter of an excited vibrational state can differ from the value of the corresponding parameter of the ground vibrational state only for some (5–10) percent. At the same time (it can be estimated, for example, on the basis of the operator perturbation theory), values of many of resonance interaction coefficients in Eqs. (4)–(8) are comparable with values of even largest centrifugal distortion parameters. On that reason, in our present analysis we tried not to change centrifugal distortion coefficients, but varied different resonance interaction parameters which have the same impact on the calculated energy values as centrifugal coefficients. The set of 77 varied parameters (18 parameters of the diagonal blocks and 59 resonance interaction parameters) is presented in Tables 6–8 together with their 1σ statistical confidence intervals (the lasts are shown in parentheses). Parameters which are presented in Tables 6–8 without parentheses were not varied and were fixed to the theoretically estimated values. For comparison, ground state parameters are given in Column 2 of Table 6. One can see more than satisfactory correspondence both between the values of fitted rotational parameters of different vibrational states, and between parameters of the excited and the ground vibrational states. Finally, a set of 77 fitted parameters reproduce the 589 initial energy values of the $(v_7 = v_{10} = 1)$ and $(v_{10} = v_{12} = 1)$ vibrational states with the $d_{rms} = 6.1 \times 10^{-4}$ cm^{-1} ($d_{rms} = 5.4 \times 10^{-4}$ cm^{-1} was obtained for the 404 ro-vibrational energies of the $(v_7 = v_{10} = 1)$ state, and $d_{rms} = 7.9 \times 10^{-4}$ cm^{-1} was obtained for the 185 ro-vibrational energies of the $(v_{10} = v_{12} = 1)$ state; see also statistical information in Table 2), that can be considered as a good confirmation of correctness of the model used. Also for illustration, column 9 of Supplementary Material and columns 4 of Tables 4 and 5 present values of differences δ (in units 10^{-4} cm^{-1}) between experimental and calculated values of line positions and ro-vibration energy values, respectively.

From the diagram, Fig. 6, one can expect the presence of numerous resonance interactions between the studied ro-vibrational states. As an illustration of the complicate picture of the appeared resonance interactions, Fig. 7 shows a small fragment of the reduced ro-vibrational energies of the lowest *g*-type vibrational states as calculated from the parameters of Tables 6–8. The crossings of curves belonging to the different vibrational states (they are marked by different colors) indicate the regions of strong local resonance interactions. The crossings agree well with peculiarities observed in the experimental spectra, thus confirming the ability of the Hamiltonian model used.

One more point should be discussed here. For the reader it can be interesting to have, at least, approximate information about uncertainties of the discussed "hot" transitions. Of course, in the frame of the present paper it is difficult to get reliable line intensities. However, to get an impression, we made approximate (only with one main dipole moment parameter) calculations of the relative line strengths in the hot band $\nu_7+\nu_{10}-\nu_{10}$ (as an illustration, see the bottom part of Fig. 4). Comparison of the simulated spectrum with the experimental data shows that both spectra correspond satisfactory to each other, and differences between experimental and calculated strength's values of the not very weak unblended lines can be estimated as 5–7%. Of course,

uncertainty is increased with the decreasing of intensity of lines, and for weakest lines which are still seen above the noise, the uncertainty of the line intensities are increased up to 60–80%.

6. Conclusion

We analyzed two weak "hot" absorption bands, $\nu_7+\nu_{10}-\nu_{10}$ and $\nu_{10}+\nu_{12}-\nu_{10}$, of the C_2H_4 molecule and assigned in the experimental spectra (spectra have been recorded with some different pressures and path lengths at the room temperature) 930 and 370 transitions (404 and 185 upper state ro-vibrational energy values) with $J^{max.}=27$, $K_a^{max.}=14$ and $J^{max.}=20$, $K_a^{max.}=9$ for the bands $\nu_7+\nu_{10}-\nu_{10}$ and $\nu_{10}+\nu_{12}-\nu_{10}$, respectively. At the theoretical analysis of the obtained results, we took into account strong local resonance interactions with 10 other ro-vibrational bands. A set of 77 varied parameters was obtained from the weighted fit, which reproduce the initial experimental data with the *rms* deviation of 6.1×10^{-4} cm^{-1} which is close to experimental uncertainties.

Acknowledgments

The work was supported by the project "Leading Russian Research Universities" (Grant FTI-120 of the Tomsk Politechnic University). Part of the work was supported by the Foundation of the President of the Russian Federation (Grant MK-4872.2014.2) and by the Deutsche Forschungsdemeinschaft (Grants BA 2176/3-2 and BA 2176/4-1).

Appendix A. Supplementary data

Supplementary data associated with this paper can be found in the online version at http://dx.doi.org/10.1016/j.jqsrt.2014.08.013.

References

[1] Abele FB, Heggetad HE. Ethylene: an urban air pollutant. J Air Pollut Control Assoc 1973;23:517–21.
[2] Betz L. Ethylene in IRC.10216. Astrophys J 1981;244:L103–5.
[3] Cernicharo J, Heras AM, Pardo JR, Tielens AGGM, Guelin M, Dartois E, et al. Methylpolyynes and small hydrocarbons in CRL 618. Astrophys J 2001;546:L127–30.
[4] Kostiuk T, Romani P, Espenak F, Livengood TA, Goldstein JJ. Temperature and abundances in the Jovian auroral stratosphere 2. Ethylene as a probe of the microbar region. J Geophys Res 1993;98:18823–30.
[5] Griffith CA, Bézard B, Greathouse TK, Kelly DM, Lacy JH, Noll KS. Thermal infrared imaging spectroscopy of Shoemaker-Levy 9 impact sites: spatial and vertical distributions of NH_3, C_2H_4, and 10-μm dust emission. Icarus 1997;128:275–93.
[6] Bezard B, Moses JL, Lacy J, Greathouse T, Richter M, Griffith C. Detection of ethylene (C_2H_4) on Jupiter and Saturn in non-auroral regions. Bull Am Astron Soc 2001;33:1079.
[7] Schulz B, Encrenaz T, Bezard B, Romani P, Lellouch E, Atreya SK. Detection of C_2H_4 in Neptune from ISO/PHTS observations. Astron Astrophys 1999;350:L13–7.
[8] Saslaw WC, Wildey RL. On the chemistry of Jupiter's upper atmosphere. Icarus 1967;7:85–93.
[9] Coustenis A, Achterberg RK, Conrath BJ, Jennings DE, Marten A, Gautier D, et al. The composition of Titan's stratosphere from Cassini/CIRS midinfrared spectra. Icarus 2007;189:35–62.
[10] Kunde VG, Aikin AC, Hanel RA, Jennings DE, Maguire WC, Samuelson RE. C4H2, HC3 N and C2N2 in Titan's atmosphere. Nature 1981;292:686–8.
[11] Bar-Nun A, Podolak M. The photochemistry of hydrocarbons in Titan's atmosphere. Icarus 1979;38:115–22.
[12] Coustenis A, Salama A, Schulz B, Ott S, Lellouch E, Encrenaz Th, et al. Titan's atmosphere from ISO mid-infrared spectroscopy. Icarus 2003;161:383–403.
[13] Vervack Jr. RJ, Sandel BR, Strobel DF. New perspectives on Titan's upper atmosphere from a reanalysis of the Voyager 1 UVS solar occultations. Icarus 2004;170:91–112.
[14] Rusinek E, Fichoux H, Khelkhal M, Herlemont F, Legrand J, Fayt A. Subdoppler study of the ν_7 band of C_2H_4 with a CO_2 laser sideband spectrometer. J Mol Spectrosc 1998;189:64–73.
[15] Tan TL, Lau SY, Ong PP, Goh KL, Teo HH. High-resolution Fourier transform infrared spectrum of the ν_{12} fundamental band of ethylene (C_2H_4). J Mol Spectrosc 2000;203:303–10.
[16] Duncan JL, Robertson GE. Vibrational anharmonicity in ethylenic compounds. J Mol Spectrosc 1991;145:251–61.
[17] Martin JML, Lee TJ, Taylor PR, François JP. The anharmonic force field of ethelene, C_2H_4, by means of accurate *ab initio* calculations. J Chem Phys 1995;103:2589–602.
[18] Ulenikov ON, Onopenko GA, Bekhtereva ES, Petrova TM, Solodov AM, Solodov AA. High resolution study of $\nu_5+\nu_{12}$ band of C_2H_4. Mol Phys 2010;108:637–47.
[19] Knippers W, Van Helvoort K, Stolte S, Reuss J. Raman overtone spectroscopy of ethylene. Chem Phys 1985;98:1–6.
[20] Loroño M, Bermejo D, Rotger M, Boudon V. High-resolution stimulated Raman spectroscopy and analysis of the $2\nu_{10}$ overtone symmetric motion of C_2H_4. J Raman Spectrosc 2004;40:1065–71.
[21] Bermejo D, Cané, Di Lonardo G, Doménech JL, Escribano R, Martinez RZ, et al. The ν_2, ν_3 and $2\nu_{10}$ Raman band of ethylene ($^{12}C_2H_4$). Mol Phys 2004;102:1659–69.
[22] Willaert F, Demaison J, Margules L, MAder H, Spahn H, Giesen T, et al. The spectrum of ethylene from microwave to submillimetre-wave. Mol Phys 2006;104:273–92.
[23] Dam N, Engeln R, Reuss J, Pine AS, Fayt A. Ethylene hot bands from molecular jet double-resonance spectroscopy. J Mol Spectrosc 1990;139:215–35.
[24] Oomens J, Reuss J, Mellau GCh, Klee S, Gulaczyk I, Fayt A. The ethylene hot band spectrum near 3000 cm^{-1}. J Mol Spectrosc 1996;180:236–48.
[25] Ahonen T, Alanko S, Horneman VM, Koivusaari M, Paso R, Tolonen AM, et al. A long path cell for the Fourier spectrometer Bruker IFS 120 HR: application to the weak $\nu_+\nu_2$ and $3\nu_2$ bands of carbon disulfide. J Mol Spectrosc 1997;181:279–86.
[26] Ulenikov ON, Gromova OV, Bekhtereva ES, Belova AS, Bauerecker S, Maul C, et al. High resolution analysis of the (111) vibrational state of SO_2. J Quant Spectrosc Radiat Transfer 2014;144:1–10.
[27] Horneman VM. High accurate peak positions for calibration purposes with the lowest fundamental bands ν_2 of N_2O and CO_2. J Mol Spectrosc 2007;241:45–50.
[28] Horneman VM. Instrumental and calculation methods for Fourier transform infrared spectroscopy and accurate standard spectra. Thesis Acta Univ Oul A 1992;239:127.
[29] Maki AG, Wells JS. Wavenumber calibration tables from heterodyne frequency measurements (version 1.3). Gaithersburg, MD: National Institute of Standards and Technology; 1998.
[30] Duncan JL, Ferguson AM. Local mode and normal mode interpretations of the CH and CD stretching vibrational manifolds in C_2H_4 and C_2D_4. J Chem Phys 1988;89:4216–26.
[31] Ulenikov ON, Tolchenov RN, Koivusaari M, Alanko S, Anttila R. High-resolution Fourier transformed spectra of CH_2D_2: pentade of the lowest interacting vibrational bands $\nu_4(A_1)$, $\nu_7(B_1)$, $\nu_9(B_2)$, $\nu_5(A_2)$, and $\nu_3(A_1)$. J Mol Spectrosc 1994;167:109–30.
[32] Ulenikov ON, Onopenko GA, Lin H, Zhang JH, Zhou ZY, Zhu QS, et al. Joint rotational analysis of 24 bands of thr H_2Se molecule. J Mol Spectrosc 1998;189:29–39.
[33] He SG, Ulenikov ON, Onopenko GA, Bekhtereva ES, Wang XH, Hu SM, et al. High-resolution Fourier transformed spectrum of the D_2O molecule in the region of the second triad of interacting vibrational states. J Mol Spectrosc 2000;200:34–9.
[34] Ulenikov ON, He SG, Onopenko GA, Bekhtereva ES, Wang XH, Hu SM, et al. High resolution study of the $(\nu_1+\frac{1}{2}\nu_2+\nu_3=3)$ Polyad of strongly interacting vibrational bands of D_2O. J Mol Spectrosc 2000;204:216–25.
[35] Zheng JJ, Ulenikov ON, Onopenko GA, Bekhtereva ES, He SG, Wang XH, et al. High resolution vibration-rotation spectrum of the D_2O

molecule in the region near the $2\nu_1+\nu_2+\nu_3$ absorption band. Mol Phys 2001;99:931–7.
[36] Ulenikov ON, Hu SM, Bekhtereva ES, Onopenko GA, Wang XH, He SG, et al. High-resolution Fourier transform spectrum of HDO in the region 6140–7040 cm^{-1}. J Mol Spectrosc 2001;208:224–35.
[37] Watson JKG. Determination of centrifugal distortion coefficients of asymmetric-top molecules. J Chem Phys 1967;46:1935–49.
[38] Ulenikov ON. On the determination of the reduced rotational operator for polyatomic molecules. J Mol Spectrosc 1986;119:144–52.
[39] Herzberg G. Molecular spectra and molecular structure, infrared and raman Spectra of polyatomic molecules, vol. 2. 1st ed.New York: van Nostrand; 1945.
[40] Ulenikov ON, Gromova OV, Aslapovskaya YuS, Horneman VM. High resolution spectroscopic study of C_2H_4: re-analysis of the ground state and ν_4, ν_7, ν_{10}, and ν_{12}, vibrational bands. J Quant Spectrosc Radiat Transfer 2013;118:14–25.
[41] Ulenikov ON, Bekhtereva ES, Albert S, Bauerecker S, Hollenstein H, Quack M. High-resolution near infrared spectroscopy and vibrational dynamics of dideuteromethane (CH_2D_2). J Phys Chem A 2009;113:2218–31.
[42] Ulenikov ON, Gromova OV, Bekhtereva ES, Bolotova IB, Leroy C, Horneman VM, Alanko S. High resolution study of the $\nu_1+2\nu_2-\nu_2$ and $2\nu_2+\nu_3-\nu_2$ "hot" bands and ro-vibrational re-analysis of the $\nu_1+\nu_2/\nu_2+\nu_3/3\nu_2$ polyad of the $^{32}SO_2$ molecule. J Quant Spectrosc Radiat Transfer, 2011;112:486–512.
[43] Ulenikov ON, Gromova OV, Bekhtereva ES, Bolotova IB, Konov IA, Horneman VM, et al. High resolution analysis of the SO_2 spectrum in the 2600–2900 cm^{-1} region: $2\nu_3$, $\nu_2+2\nu_3-\nu_2$ and $2\nu_1+\nu_2$ bands. J Quant Spectrosc Radiat Transfer 2012;113:500–17.
[44] Ulenikov ON, Onopenko GA, Gromova OV, Bekhtereva ES, Horneman VM. Re-analysis of the (100), (001), and (020) rotational structure of SO_2 on the basis of high resolution FTIR spectra. J Quant Spectrosc Radiat Transfer 2013;130:220–32.
[45] Papousek D, Aliev MR. Molecular vibrational–rotational spectra. Amsterdam: Elsevier; 1982.